# AFRL-VA-WP-TR-2000-3049

# NONLINEAR RANDOM RESPONSE OF COMPOSITE PANELS IN AN ELEVATED THERMAL ENVIRONMENT

C. MEI
J.M. DHAINAUT
B. DUAN
CAPT. S.M. SPOTTSWOOD
H.F. WOLFE


OLD DOMINION UNIVERSITY
P.O. BOX 6369
NORFOLK, VA 23509-0369

## OCTOBER 2000

**FINAL REPORT FOR PERIOD 04 DECEMBER 1999 – 13 OCTOBER 2000**

20010417 023

AIR VEHICLES DIRECTORATE
AIR FORCE RESEARCH LABORATORY
AIR FORCE MATERIEL COMMAND
WRIGHT-PATTERSON AIR FORCE BASE, OH 45433-7542
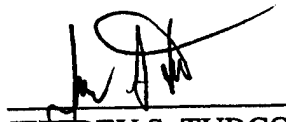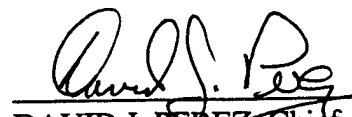
# NOTICE

USING GOVERNMENT DRAWINGS, SPECIFICATIONS, OR OTHER DATA INCLUDED IN THIS DOCUMENT FOR ANY PURPOSE OTHER THAN GOVERNMENT PROCUREMENT DOES NOT IN ANY WAY OBLIGATE THE US GOVERNMENT. THE FACT THAT THE GOVERNMENT FORMULATED OR SUPPLIED THE DRAWINGS, SPECIFICATIONS, OR OTHER DATA DOES NOT LICENSE THE HOLDER OR ANY OTHER PERSON OR CORPORATION; OR CONVEY ANY RIGHTS OR PERMISSION TO MANUFACTURE, USE, OR SELL ANY PATENTED INVENTION THAT MAY RELATE TO THEM.

THIS REPORT IS RELEASABLE TO THE NATIONAL TECHNICAL INFORMATION SERVICE (NTIS). AT NTIS, IT WILL BE AVAILABLE TO THE GENERAL PUBLIC, INCLUDING FOREIGN NATIONS.

THIS TECHNICAL REPORT HAS BEEN REVIEWED AND IS APPROVED FOR PUBLICATION.

S. MICHAEL SPOTTSWOOD, Capt, USAF
Structural Engineer
Structural Dynamics Branch

DAVID J. PEREZ, Chief
Structural Dynamics Branch
Structures Division

JEFFREY S. TURCOTTE, Lt Col, USAF
Deputy Chief, Structures Division
Air Vehicles Directorate

Do not return copies of this report unless contractual obligations or notice on a specific document requires its return.

# REPORT DOCUMENTATION PAGE

*Form Approved*
*OMB No. 0704-0188*

| 1. AGENCY USE ONLY (Leave blank) | 2. REPORT DATE<br><br>October 2000 | 3. REPORT TYPE AND DATES COVERED<br>FINAL 12/4/99 – 10/13/00 |
|---|---|---|

| 4. TITLE AND SUBTITLE<br>Nonlinear Random Response of Composite Panels in an Elevated Thermal Environment | 5. FUNDING NUMBERS<br>CF33615-98-D-3210<br>E 60110 2<br>PR 2302<br>TA N0<br>WU 02 |
|---|---|
| 6. AUTHOR (S)<br>C. Mei, Principal Investigator<br>J.M. Dhainaut and B. Duan, Graduate Research Assistants<br>Capt. S.M. Spottswood, USAF & H.F. Wolfe, Senior Aerospace Engineer | |

| 7. PERFORMING ORGANIZATION NAME(S) AND ADDRESS(ES)<br>Old Dominion University<br>P.O. Box 6369<br>Norfolk, VA 23509-0369 | 8. PERFORMING ORGANIZATION REPORT NUMBER |
|---|---|

| 9. SPONSORING/MONITORING AGENCY NAME(S) AND ADDRESS(ES)<br>Air Vehicles Directorate<br>Air Force Research Laboratory<br>Air Force Materiel Command<br>Wright-Patterson AFB, OH 45433-7542<br>POC: Capt. S. Michael Spottswood, AFRL/VASS 937-255-5200 x457 | 10. SPONSORING/MONITORING AGENCY REPORT NUMBER<br><br>AFRL-VA-WP-TR-2000-3049 |
|---|---|

**11. SUPPLEMENTARY NOTES**

| 12a. DISTRIBUTION AVAILABILITY STATEMENT<br>Approved for public release; distribution unlimited | 12b. DISTRIBUTION CODE |
|---|---|

**13. ABSTRACT** *(Maximum 200 words)*

Sonic fatigue is being considered as one of the major design parameters for the new generation of high-speed flight vehicles. Efficient and accurate analysis methods for predicting nonlinear random response and estimating fatigue life of surface panels are urgently needed. A brief review of the various analysis methods for nonlinear random vibrations of aircraft surface panels is given. An efficient finite element modal formulation is presented for the prediction of panel response at high sound pressure levels and elevated temperatures. Band-limited Gaussian white noise is generated as input excitation. Numerical results were compared with linear analytical and Fokker-Planck-Kolmogorov equation solutions for validation of the present method. Number of modes, mesh size, and integration time steps for accurate and converged response predictions were also presented. Examples are given for a simply supported isotropic and a clamped composite panel at various combinations of sound pressure level and temperature. Numerical results include time-histories, root mean square values of maximum deflection and strain, probability distribution functions, power spectrum densities (PSD), and higher statistical moments of maximum deflection and strain. The PSD can be used for fatigue life estimation.

| 14. SUBJECT TERMS<br>Sonic Fatigue, Random Response, Fatigue and Acoustics | | 15. NUMBER OF PAGES<br>58 |
|---|---|---|
| | | 16. PRICE CODE |

| 17. SECRITY CLASSIFICATION OF REPORT<br><br>Unclassified | 18. SECURITY CLASSIFICATION OF THIS PAGE<br><br>Unclassified | 19. SECURITY CLASSIFICATION OF ABSTRACT<br><br>Unclassified | 20. LIMITATION OF ABSTRACT<br><br>SAR |
|---|---|---|---|

Standard Form 298 (Rev. 2-89) (EG)
Prescribed by ANSI Std. 239. 18
Designed using Perform Pro, WHS/DIOR,

# Table of Contents

# List of Figures

# List of Tables

# Acknowledgement

# 1. Introduction

Sonic fatigue has been considered as one of the major design considerations for the Joint Strike Fighter (JSF). In addition, the surface panels of many high-speed flight vehicles (e.g., the X-33, RLV, X-38, and X-43, etc.) presently under development will be exposed to high levels of acoustic pressure and elevated temperatures. This brings an urgent need for the sonic fatigue analysis and design methods for aircraft and spacecraft structural panels.

For safety and reliability, the design of modern structures such as skyscraper buildings, constructions housing nuclear reactors, and naval and aerospace structures must take into consideration various intense random excitations. These excitations include seismic motions of earthquakes, pressure waves of explosions or blasts, jet noise, and atmospheric turbulence. The three important aerospace problems of random vibration [1] are the following: buffeting of aircraft by atmospheric turbulence, sonic fatigue of aircraft and spacecraft panels due to jet noise impingement or boundary layer pressure fluctuations, and the reliability of payloads in rocket-propelled vehicles.

## 1.1 Nonlinear Random Vibration Analysis Techniques

Stochastically excited linear systems have been studied in great detail and numerous analytical techniques exist for both stationary and nonstationary problems. Unfortunately, the majority of structural responses are nonlinear and not many techniques exist for the analysis. Crandall and Zhu [1], To [2], Roberts [3], and Spanos and Lutes [4] have presented excellent and comprehensive reviews on techniques for nonlinear random vibrations. The various approaches are given briefly in the following paragraphs.

### 1.1.1 Fokker-Planck-Kolmogorov (FPK) Equations Approaches

The FPK equations approaches give an exact solution for a restricted class of simple problems. The most general extension of FPK equations approaches to nonlinear second

order equations was due to Caughey [5]. Exact steady-state solutions of rather wide class of Multi-Degrees-of-Freedom (MDOF) nonlinear systems to white noise are available [6,7]. In general, the transitional Probability Density Function (PDF) cannot be found with the FPK equation approach. Without this transitional probability, it is generally impossible to obtain the correlation function and Power Spectral Density (PSD) of the response. The difficulty in dealing exactly with solutions of stochastically excited nonlinear systems has led to an intensified effort to develop approximate methods, to tackle a broader class of problems than presently possible with the exact analysis.

## 1.1.2 Perturbation Approaches

In this approximate method, the stochastically exited nonlinear system is treated in the same way as a deterministically excited system. The solution is represented as an expansion of the powers of a small parameter which specifies the size of the nonlinearity. The perturbation approach was applied to a continuous nonlinear system by Lyon [8] and to discrete nonlinear systems by Crandall [9]. The perturbation approximation; however, will not give accurate result for systems of large nonlinearity [10] as shown in Figure 1.

## 1.1.3 Equivalent Linearization (EL) Approaches

The EL approaches technique is based on the concept of replacing the nonlinear system by an equivalent linear system such that the difference between the two systems is minimized. Basically, the method is the statistical extension of well-known Krylov-Bogoliubov equivalent linearization method for deterministic vibration problems. The extension of this approximate method to problems of random excitations was made independently by Booton [11] and Caughey [12]. Atalik and Utku [13] have presented a direct and generalized procedure of the equivalent linearization approach for the MDOF nonlinear systems that may be nonlinear in inertial, velocity, and restoring forces. The coefficients of the equivalent linear system can be obtained by direct application of partial differentiation and expectation operators to the functionals involving nonlinear terms. For mathematical derivations of the equivalent linearization technique and its

2

applications to the variety of nonlinear dynamic systems, the readers are referred to the published book by Roberts and Spanos [14].

### 1.1.4 Numerical Simulation Approaches

Simulation or the Monte Carlo method estimates the response statistics of randomly excited nonlinear structural systems [15-17]. In the past, both analog and digital computational systems have been used for Monte Carlo simulations. Only digital systems are used presently. The approach mainly consists of generating a large number of sample excitations, calculating the corresponding response samples, and processing the desired response statistics. Obviously, this approach can be used for estimating the response statistics of both stationary and nonstationary excitations. The major drawback of this approach is the computation time and cost.

The various analysis techniques discussed for nonlinear random vibration systems in Section 1.1 were not dealt with thermal environment. A brief review of sonic fatigue analysis and design methods for aircraft and spacecraft structural panels in a combined thermal acoustic environment is presented.

### 1.2 Nonlinear Random Response of Panels in an Elevated Thermal Environment

Sonic fatigue design guides have been developed for metallic structures by Rudder and Plumblee [18] and for graphite-epoxy composite structures by Holehouse [19]. The design guides were based on the semi-empirical test data or the simplified single-mode Miles' approach.

Vaicaitis and his coworkers have used the Galerkin's method (to Partial Differential Equations (PDE) and modal approach) in conjunction with the time domain Monte Carlo numerical simulation [15-17] for the prediction of nonlinear response of isotropic [20,21] and composite [22,23] panels subjected to acoustic and thermal loads. Lee [24-26] has used the PDE/Galerkin method in conjunction with the equivalent linearization [14]

3

technique and investigated the thermal effects on the dynamics of vibrating isotropic plates and the improvement of variance and cumulants using the abridged Edgeworth series [27]. The use of the PDE/Galerkin method, however, limits its applicability to simple panel planform of rectangular shape and simple boundary conditions.

Extension of the Finite Element (FE) method to nonlinear response of isotropic beam [28] and plate [29] structures under combined acoustic and thermal loads was first reported by Locke and Mei using the EL technique with an iterative scheme. The application of the FE/EL procedure was further extended to composite panels by Mei and Chen [30]. In the FE/EL solution procedure, the thermal postbuckling or thermal finite deflection structural problem is solved first. The thermal deflection and thermal stresses are treated as known preconditions for the subsequent random response analysis. The random response thus considers only one of the two coexisting thermal postbuckling positions [31]. The FE/EL method, therefore, does not give accurate predictions for snap-through (or oil-canning) and large-amplitude nonlinear random motions. Experiments by Ng and Clevenson [32], Istenes et al. [33], and Murphy et al. [34, 35] have shown that the dynamic response of acoustic excited thermally buckled plates may exhibit the following two types of motion: (i) small amplitude vibrations about one of the coexisting static equilibriums, and (ii) large amplitude nonlinear snap-through oscillations between and over the two postbuckling positions. Reviews of large deflection analysis in sonic fatigue design were given by Mei and Wolfe [36], Benaroya and Rebak [37], Vaicaitis [20, 21], Clarkson [38], and Wolfe et al. [39].

This report presents an efficient finite element method for the prediction of nonlinear random response of composite panels at elevated temperatures. The system equations of motion are first derived in the structural node degree of freedom (DOF), then they are reduced to a set of coupled nonlinear modal equations. Numerical integration is used to obtain the panel response. The following three types of motions can be predicted: (i) linear random vibration about one of the thermally buckled position, (ii) snap-through between the two buckled positions, and (iii) nonlinear random vibration over the two thermally buckled positions. Examples are given for an isotropic plate and a composite plate.

$$s(y_i) = ky_i + \mu y_i^3$$

$$\sigma_{y_i}(\mu=0) = (\lambda/2ck)^{1/2}$$

$\dfrac{\sigma_{y_i}}{\sigma_{y_i}(\mu=0)}$

Exact solution

Perturbation approach

Statistical linearization approach

$\dfrac{\mu}{k}[\sigma_{y_i}(\mu=0)]^2$
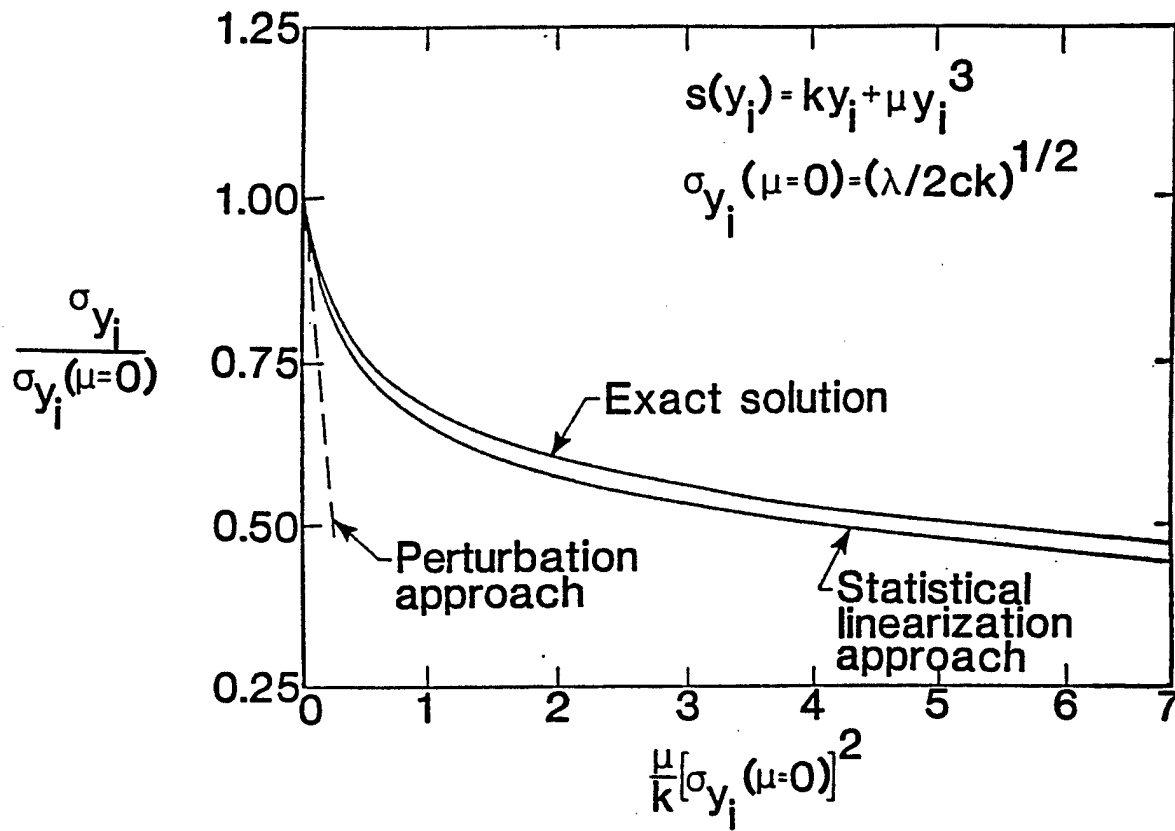
**Figure 1.** RMS Responses of a Hardening System by

Perturbation, EL and FPK Approaches (Iwan & Yang, 1972)

## 2. Finite Element Formulation

The governing nonlinear equations of motion are derived for an arbitrarily laminated composite plate subjected to a set of simultaneously applied thermal and acoustic loads. The thermal load is taken to be an arbitrary distribution and steady-state, i.e., $\Delta T = \Delta T(x,y,z)$. The acoustic excitation is assumed to be a band-limited Gaussian random noise and uniformly distributed over the structural surface.

### 2.1 Equations of Motion in Structural Node DOF

The element displacements are expressed in terms of the node DOF as

$$
\begin{aligned}
u(x,y,t) &= \lfloor H_u \rfloor \{w_m\} \\
v(x,y,t) &= \lfloor H_v \rfloor \{w_m\} \\
w(x,y,t) &= \lfloor H_w \rfloor \{w_b\}
\end{aligned}
\tag{1}
$$

where $u$, $v$, and $w$ are the in-plane and transverse displacements of the middle surface; the vectors $\{w_m\}$ and $\{w_b\}$ denote the in-plane and bending node DOF; and $\lfloor H_u \rfloor$, $\lfloor H_v \rfloor$, and $\lfloor H_w \rfloor$ denote in-plane and transverse displacement functions, respectively.

The finite element formulation is based on the von Karman large deflection and the laminated plate theories. The strain-displacement relations are given

$$
\{\varepsilon\} = \left\{ \begin{array}{c} \varepsilon_x \\ \varepsilon_y \\ \gamma_{xy} \end{array} \right\} = \{\varepsilon^0\} + z\{\kappa\} = \{\varepsilon_m^0\} + \{\varepsilon_\theta^0\} + z\{\kappa\}
\tag{2}
$$

and

$$
\{\varepsilon_m^0\} = \left\{ \begin{array}{c} u_{,x} \\ v_{,y} \\ u_{,y} + v_{,x} \end{array} \right\} = [B_m]\{w_m\}
\tag{3}
$$

$$\{\varepsilon_\theta^0\} = \frac{1}{2} \begin{Bmatrix} w_{,x}^2 \\ w_{,y}^2 \\ 2w_{,x}w_{,y} \end{Bmatrix} = \frac{1}{2} \begin{bmatrix} w_{,x} & 0 \\ 0 & w_{,y} \\ w_{,y} & w_{,x} \end{bmatrix} \begin{Bmatrix} w_{,x} \\ w_{,y} \end{Bmatrix} = \frac{1}{2}[\theta][B_\theta]\{w_b\} \tag{4}$$

$$\{\kappa\} = \begin{Bmatrix} -w_{,xx} \\ -w_{,yy} \\ -2w_{,xy} \end{Bmatrix} = [B_b]\{w_b\} \tag{5}$$

where $\{\varepsilon^0\}$ and $\{\kappa\}$ denote the in-plane strain and curvature strain vectors; and $[\theta]$ is the slope matrix, respectively. The matrices $[B_m]$, $[B_\theta]$, and $[B_b]$ are the strain interpolation matrices corresponding to in-plane, large deflection, and bending strain components, respectively. The subscripts $m$, $\theta$, and $b$ denote that the strain components are due to membrane, large deflection, and bending, respectively; and the comma denotes the derivative.

The linear constitutive relations for the $k^{th}$ orthotropic lamina in the principal material coordinates are

$$\begin{Bmatrix} \sigma_1 \\ \sigma_2 \\ \tau_{12} \end{Bmatrix}_k = \begin{bmatrix} Q_{11} & Q_{12} & 0 \\ Q_{12} & Q_{22} & 0 \\ 0 & 0 & Q_{66} \end{bmatrix}_k \left( \begin{Bmatrix} \varepsilon_1 \\ \varepsilon_2 \\ \gamma_{12} \end{Bmatrix} - \begin{Bmatrix} \alpha_1 \\ \alpha_2 \\ 0 \end{Bmatrix}_k \Delta T \right) \tag{6}$$

where $[Q]$ is the reduced stiffness matrix of the composite lamina, and $\{\alpha\}_k$ is the coefficient of thermal expansion. The terms in $[Q]$ can be evaluated as follows:

$$Q_{11} = \frac{E_1}{1 - v_{12}v_{21}}$$

$$Q_{12} = \frac{v_{12}E_2}{1 - v_{12}v_{21}} = \frac{v_{21}E_1}{1 - v_{12}v_{21}} \tag{7}$$

$$Q_{22} = \frac{E_2}{1 - v_{12}v_{21}}$$

$$Q_{66} = G_{12}$$

Consider the composite lamina having an arbitrary orientation angle $\phi$, the stress and strain transformation relations from the principal directions 1, 2 to x, y body directions are:

$$\begin{Bmatrix} \sigma_1 \\ \sigma_2 \\ \tau_{12} \end{Bmatrix} = [T_\sigma(\phi)] \begin{Bmatrix} \sigma_x \\ \sigma_y \\ \tau_{xy} \end{Bmatrix}, \qquad \begin{Bmatrix} \varepsilon_1 \\ \varepsilon_2 \\ \gamma_{12} \end{Bmatrix} = [T_\varepsilon(\phi)] \begin{Bmatrix} \varepsilon_x \\ \varepsilon_y \\ \gamma_{xy} \end{Bmatrix} \qquad (8)$$

where

$$[T_\sigma(\phi)] = \begin{bmatrix} c^2 & s^2 & 2sc \\ s^2 & c^2 & -2sc \\ -sc & sc & c^2 - s^2 \end{bmatrix}, \qquad [T_\varepsilon(\phi)] = \begin{bmatrix} c^2 & s^2 & sc \\ s^2 & c^2 & -sc \\ -2sc & 2sc & c^2 - s^2 \end{bmatrix} \qquad (9)$$

with $c=\cos(\phi)$, $s=\sin(\phi)$.

Thus, the stress-strain relations for a general $k^{th}$ lamina with an orientation angle $\phi$ and a temperature change become:

$$\{\sigma\}_k = \begin{Bmatrix} \sigma_x \\ \sigma_y \\ \tau_{xy} \end{Bmatrix}_k = \begin{bmatrix} \overline{Q}_{11} & \overline{Q}_{12} & \overline{Q}_{16} \\ \overline{Q}_{21} & \overline{Q}_{22} & \overline{Q}_{26} \\ \overline{Q}_{61} & \overline{Q}_{62} & \overline{Q}_{66} \end{bmatrix}_k \left( \begin{Bmatrix} \varepsilon_x \\ \varepsilon_y \\ \gamma_{xy} \end{Bmatrix} - \Delta T \begin{Bmatrix} \alpha_x \\ \alpha_y \\ \alpha_{xy} \end{Bmatrix}_k \right) \qquad (10)$$

or

$$\{\sigma\}_k = [\overline{Q}]_k \left( \{\varepsilon\} - \Delta T \{\alpha\}_k \right) \qquad (11)$$

where $[\overline{Q}]_k$ the transformed reduced stiffness matrix is given by,

$$[\overline{Q}]_k = [T_\sigma(\phi)]^{-1} [Q][T_\varepsilon(\phi)] \qquad (12)$$

The resultant forces and moments per unit length are

$$\left( \{N\} \, , \, \{M\} \right) = \int_{-h/2}^{h/2} \{\sigma\}_k (1, z) dz \tag{13}$$

and the constitutive equations for a laminate can be written as

$$\begin{Bmatrix} N \\ M \end{Bmatrix} = \begin{bmatrix} A & B \\ B & D \end{bmatrix} \begin{Bmatrix} \varepsilon^o \\ \kappa \end{Bmatrix} - \begin{Bmatrix} N_{\Delta T} \\ M_{\Delta T} \end{Bmatrix} \tag{14}$$

where $[A]$, $[B]$, and $[D]$ are the laminate extensional, extension-bending, and bending stiffness matrices, respectively. The vectors $\{N_{\Delta T}\}$ and $\{M_{\Delta T}\}$ are the in-plane force and moment due to thermal expansion

$$\left( \{N_{\Delta T}\} \, , \, \{M_{\Delta T}\} \right) = \int_{-h/2}^{h/2} [\overline{Q}]_k \Delta T \{\alpha\}_k (1, z) dz \tag{15}$$

Using the principle of virtual work, the element nonlinear equations of motion are derived with the internal and external virtual work as

$$\delta W_{\text{int}} = \int_A \left( \{\delta \varepsilon^o\}^T \{N\} + \{\delta \kappa\}^T \{M\} \right) dA$$
$$\delta W_{ext} = \int_A \{\delta w \left( p(x,y,t) - \rho h w_{,tt} \right) - \delta u \left( \rho h u_{,tt} \right) - \delta v \left( \rho h v_{,tt} \right)\} dA \tag{16}$$

and the element equations of motion can be expressed as

$$\begin{bmatrix} m_b & 0 \\ 0 & m_m \end{bmatrix} \begin{Bmatrix} \ddot{w}_b \\ \ddot{w}_m \end{Bmatrix} + \left( \begin{bmatrix} k_b & k_B \\ k_B^T & k_m \end{bmatrix} - \begin{bmatrix} k_{N\Delta T} & 0 \\ 0 & 0 \end{bmatrix} \right) \begin{Bmatrix} w_b \\ w_m \end{Bmatrix}$$

$$+ \left( \begin{bmatrix} k_{1Nm} + k_{1NB} & k_{1bm} \\ k_{1mb} & 0 \end{bmatrix} + \begin{bmatrix} k_{2b} & 0 \\ 0 & 0 \end{bmatrix} \right) \begin{Bmatrix} w_b \\ w_m \end{Bmatrix} = \begin{Bmatrix} p_{b\Delta T} \\ p_{m\Delta T} \end{Bmatrix} + \begin{Bmatrix} p_b(t) \\ 0 \end{Bmatrix} \tag{17}$$

9

The element matrices and load vectors are listed in Appendix A. The subscripts B, N$\Delta$T, Nm and NB denote that the corresponding stiffness matrix is due to the laminate extension-bending $[B]$, in-plane force components $\{N_{\Delta T}\}$, $\{N_m\} = [A]\{\varepsilon_m^0\}$, and $\{N_B\} = [B]\{k\}$, respectively.

Assembling all the elements and taking into account the kinematic boundary conditions, the system equations of motion in structural node DOF can be expressed as

$$\begin{bmatrix} M_b & 0 \\ 0 & M_m \end{bmatrix}\begin{Bmatrix} \ddot{W}_b \\ \ddot{W}_m \end{Bmatrix} + \left( \begin{bmatrix} K_b & K_B \\ K_B^T & K_m \end{bmatrix} - \begin{bmatrix} K_{N\Delta T} & 0 \\ 0 & 0 \end{bmatrix} \right)\begin{Bmatrix} W_b \\ W_m \end{Bmatrix}$$

$$(18a)$$

$$+ \left( \begin{bmatrix} K_{1Nm} + K_{1NB} & K_{1bm} \\ K_{1mb} & 0 \end{bmatrix} + \begin{bmatrix} K_{2b} & 0 \\ 0 & 0 \end{bmatrix} \right)\begin{Bmatrix} W_b \\ W_m \end{Bmatrix} = \begin{Bmatrix} P_{b\Delta T} \\ P_{m\Delta T} \end{Bmatrix} + \begin{Bmatrix} P_b(t) \\ 0 \end{Bmatrix}$$

or

$$[M]\{\ddot{W}\} + ([K] - [K_{N\Delta T}] + [K_1] + [K_2])\{W\} = \{P_{\Delta T}\} + \{P(t)\} \qquad (18b)$$

where $[M]$, $[K]$, and $\{P\}$ denote the system mass, linear stiffness matrices, and load vector, respectively; and $[K_1]$ and $[K_2]$ denote the first-order and second-order nonlinear stiffness matrices which depend linearly and quadratically on displacement $\{W\}$.

For a given temperature rise $\Delta T$, Equation (18) can be solved by numerical integration in the structural node DOF with simulated random loads. This approach has been carried out for random response analysis with simulated random loads by Green and Killey [40] and Robinson [41]. It turned out to be computationally costly because of the following: (i) the large number of DOF of the system, (ii) the nonlinear stiffness matrices $[K_1]$ and $[K_2]$ have to be assembled and updated from the element nonlinear stiffness matrices at each time step, and (iii) the time step of integration has to be extremely small. Consequently, Equation (18) is transformed into a set of truncated modal coordinates with rather small DOF.

10

## 2.2 Equations of Motion in Modal Coordinates

### 2.2.1 Symmetric Laminates

For symmetrically laminated composite and isotropic panels, the laminate coupling stiffness $[B]$ is null and the two submatrices in Equation (18) are

$$[K_B] = [K_{1NB}] = 0 \tag{19}$$

By neglecting the membrane inertia term, the membrane displacement vector can be expressed in terms of the bending displacement vector as

$$\{W_m\} = [K_m]^{-1}(\{P_{m\Delta T}\} - [K_{1mb}]\{W_b\}) \tag{20}$$

Then Equation (18) can be written in terms of the bending displacement as

$$[M_b]\{\ddot{W}_b\} + ([K_b] - [K_{N\Delta T}])\{W_b\} + [K_{1bm}][K_m]^{-1}\{P_{m\Delta T}\}$$

$$+ [K_{1Nm}]\{W_b\} + ([K_{2b}] - [K_{1bm}][K_m]^{-1}[K_{1mb}])\{W_b\} = \{P_{b\Delta T}\} + \{P_b(t)\} \tag{21}$$

In the above system, the nonlinear stiffness matrices can be expressed in terms of modal coordinates. This is accomplished by expressing the panel response as a linear combination of some base functions (modal transformation) as

$$\{W_b\} = \sum_{r=1}^{n} q_r(t)\{\phi_b\}^{(r)} = [\phi]\{q\} \tag{22}$$

where $\{\phi_b\}^{(r)}$ corresponds to the normal modes of the linear vibration problem

$$\omega_r^2[M_b]\{\phi_b\}^{(r)} = [K_b]\{\phi_b\}^{(r)} \tag{23}$$

The nonlinear stiffness matrices $[K_{1bm}]$ and $[K_{2b}]$ are both in function of $\{W_b\}$. They can be expressed as the sum of products of modal coordinates and nonlinear modal stiffnesses matrices as

$$[K_{1bm}] = [K_{1mb}]^T = \sum_{r=1}^{n} q_r(t)[K_{1bm}(\phi_b)]^{(r)}$$

$$[K_{2b}] = \sum_{r=1}^{n}\sum_{s=1}^{n} q_r(t)q_s(t)[K_{2b}\phi_b]^{(rs)} \qquad (24)$$

where the super indexes of those non-linear modal stiffness matrices denote that they are assembled from the corresponding element non-linear stiffness matrices (see Appendix A). Those non-linear stiffness matrices are evaluated with the corresponding element components $\{w_b\}^{(r)}$ obtained from the known system mode $\{\phi_b\}^{(r)}$.

The nonlinear stiffness matrix $[K_{1Nm}]$ is linearly dependent on the displacement $\{W_m\}$. Recalling the membrane displacement vector of Equation (20)

$$\begin{aligned}
\{W_m\} &= [K_m]^{-1}\left(\{P_{m\Delta T}\} - [K_{1mb}]\{W_b\}\right)\\
&= [K_m]^{-1}\left(\{P_{m\Delta T}\} - \sum_{r=1}^{n}\sum_{s=1}^{n} q_r(t)q_s(t)[K_{1mb}]^{(r)}\{\phi_b\}^{(s)}\right) \qquad (25)\\
&= \{W_m\}_{\Delta T} - \sum_{r=1}^{n}\sum_{s=1}^{n} q_r(t)q_s(t)\{\phi_m\}^{(rs)}
\end{aligned}$$

It is observed that $[K_{1Nm}]$ is the sum of two matrices, the first $[K_{Nm}]_{\Delta T}$ is evaluated with $\{W_m\}_{\Delta T}$ $(=[K_m]^{-1}\{P_{m\Delta T}\})$ and the second $[K_{2Nm}]$ is evaluated with $\{\phi_m\}^{(rs)}$ $(=[K_m]^{-1}$ $[K_{1mb}]^{(r)}\{\phi_b\}^{(s)})$ as

$$[K_{1Nm}] = [K_{Nm}]_{\Delta T} - \sum_{r=1}^{n}\sum_{s=1}^{n} q_r(t)q_s(t)[K_{2Nm}(\phi_m)]^{(rs)} \qquad (26)$$

12

Introducing a structural modal damping $2\xi_r\omega_r\overline{M}_r[I]$, where the modal damping, $\xi_r$, can be determined experimentally or pre-selected from a similar structure. The equations of motion Equation (21) are reduced to a set of coupled modal equations as

$$\left[\overline{M}\right]\{\ddot{q}\}+2\xi_r\omega_r\overline{M}_r[I]\{\dot{q}\}+\left(\left[\overline{K}_L\right]+\left[\overline{K}_{qq}\right]\right)\{q\}=\{\overline{P}\} \tag{27}$$

where the diagonal modal mass is

$$\left[\overline{M}\right]=\left[\phi\right]^T\left[M_b\right]\left[\phi\right]=\overline{M}_r[I] \tag{28}$$

the linear and cubic terms are

$$\left[\overline{K}_L\right]\{q\}=\left[\phi\right]^T\left(\left[K_b\right]-\left[K_{N\Delta T}\right]+\left[K_{Nm}\right]_{\Delta T}\right)\left[\phi\right]\{q\}+\left[\phi\right]^T\sum_{r=1}^{n}q_r\left[K_{1bm}\right]^{(r)}\{W_m\}_{\Delta T} \tag{29}$$

$$\left[\overline{K}_{qq}\right]\{q\}=\left[\phi\right]^T\sum_{r=1}^{n}\sum_{s=1}^{n}q_rq_s\left(\left[K_{2b}\right]^{(rs)}-\left[K_{2Nm}\right]^{(rs)}-\left[K_{1bm}\right]^{(r)}\left[K_m\right]^{-1}\left[K_{1mb}\right]^{(s)}\right)\left[\phi\right]\{q\} \tag{30}$$

and the modal thermal and random load vector is

$$\{\overline{P}\}=\left[\phi\right]^T\left(\{P_{b\Delta T}\}+\{P_b(t)\}\right) \tag{31}$$

The nonlinear random response for a given symmetric composite or isotropic panel at certain temperature can thus be determined from Equation (27) by numerical integration scheme. The advantages of using the modal equations are the following: (i) the number of modal equations is small (DOF of $\{q\}$<<DOF of $\{W_b\}$), (ii) there is no need to assemble and update the nonlinear cubic term at each time step since all the nonlinear modal stiffness matrices are constant matrices, and (iii) the time step of integration could be larger.

13

## 2.2.2 Unsymmetric Laminates

For unsymmetrically laminated composite panels, the laminate coupling stiffness $[B] \neq 0$ which leads to the two submatrices $[K_B]$ and $[K_{INB}]$ both are not zero. The linear vibration from Equation (18) becomes

$$\omega_r^2 \begin{bmatrix} M_b & 0 \\ 0 & M_m \end{bmatrix} \begin{Bmatrix} \phi_b \\ \phi_m \end{Bmatrix}^{(r)} = \begin{bmatrix} K_b & K_B \\ K_B^T & K_m \end{bmatrix} \begin{Bmatrix} \phi_b \\ \phi_m \end{Bmatrix}^{(r)} \tag{32}$$

The bending $\{\phi_b\}^{(r)}$ and in-plane $\{\phi_m\}^{(r)}$ modes are thus coupled.

Follow the procedures for the symmetric laminates, the panel response is expressed as

$$\{W\} = \begin{Bmatrix} W_b \\ W_m \end{Bmatrix} = \sum_{r=1}^{n} q_r(t) \begin{Bmatrix} \phi_b \\ \phi_m \end{Bmatrix}^{(r)} = [\phi]\{q\} \tag{33}$$

The nonlinear stiffness matrices $[K_1]$ and $[K_2]$ can be expressed as the sum of products of modal coordinates and nonlinear modal stiffness matrices as

$$[K_1] = \sum_{r=1}^{n} q_r(t) \begin{bmatrix} [K_{1Nm}(\phi_m)]^{(r)} + [K_{1NB}(\phi_b)]^{(r)} & [K_{1bm}(\phi_b)]^{(r)} \\ [K_{1mb}(\phi_b)]^{(r)} & 0 \end{bmatrix}$$

$$= \sum_{r=1}^{n} q_r(t)[K_1]^{(r)} \tag{34}$$

and

$$[K_2] = \sum_{r=1}^{n} \sum_{s=1}^{n} q_r(t)q_s(t)[K_{2b}(\phi_b)]^{(rs)} \tag{35}$$

where the super indexes of those nonlinear modal stiffness matrices denote that they are assembled from the corresponding element nonlinear stiffness matrices. The element nonlinear stiffness matrices are evaluated with the corresponding element components

14

$\{w_b\}^{(r)}$ and $\{w_m\}^{(r)}$ obtained from the known system modes $\{\phi_b\}^{(r)}$ and $\{\phi_m\}^{(r)}$, respectively.

With the introducing a structural modal damping $2\xi_r\omega_r\overline{M}_r[I]$, equations of motion Equation (18) reduce to a set of coupled modal equations as

$$[\overline{M}]\{\ddot{q}\} + 2\xi_r\omega_r\overline{M}_r[I]\{\dot{q}\} + ([\overline{K}_L] + [\overline{K}_q] + [\overline{K}_{qq}])\{q\} = \{\overline{P}\} \tag{36}$$

where the diagonal modal mass and linear stiffness matrices are

$$([\overline{M}],[\overline{K}_L]) = [\phi]^T([M],[K - K_{N\Delta T}])[\phi] \tag{37}$$

the quadratic and cubic terms are

$$[\overline{K}_q]\{q\} = [\phi]^T \sum_{r=1}^{n} q_r[K_1]^{(r)}[\phi]\{q\} \tag{38}$$

$$[\overline{K}_{qq}]\{q\} = [\phi]^T \sum_{r=1}^{n}\sum_{s=1}^{n} q_r q_s[K_{2b}]^{(rs)}[\phi]\{q\} \tag{39}$$

and the modal thermal and random load vector is

$$\{\overline{P}\} = [\phi]^T(\{P_{\Delta T}\} + \{P(t)\}) \tag{40}$$

The nonlinear random response for a given unsymmetric composite panel at certain temperature can then be determined from Equation (36), using numerical integration. The advantages are as follows: (i) DOF of $\{q\}$ is small, (ii) no need to assemble and update the nonlinear quadratic and cubic terms, and (iii) the time step of integration could be larger.

## 2.3 Stress and Strain Calculations

After the modal displacement $\{q\}$ for a given combination of acoustic load and elevated temperature case is determined, $\{W_b\}$ and $\{W_m\}$ can be evaluated with Equation (22) and Equation (25) for the symmetric and Equation (33) for the unsymmetric panels, respectively. The element in-plane strain $\{\varepsilon^0\}$ and curvature $\{\kappa\}$ can be calculated using Equation (3) to Equation (5), respectively. The element strains are then obtained from Equation (2), and stresses for the $k^{th}$ layer are obtained using Equation (10). Stress and strain in the material principal directions are then obtained using Equation (8). For the displacement based finite element method, the stress/strain calculation is not as accurate as displacement calculation. According to Barlow [42], and Cook et al. [43], the stresses at Barlow points are calculated and the result is extrapolated to the nodal points or other desired points. The global stresses and strains are averaged from different local nodal values, which share the same global node number.

# 3. Results and Discussions

## 3.1 Uniform Distribution Random Pressure

Consider a random pressure p(x,y,t) acting on the surface of a high-speed flight vehicle. The pressure acting normal to the panel surface varies randomly in time and space along the surface coordinates x and y. The pressure p(x,y,t) is characterized by a cross-spectral density function $S_p(\xi, \eta, \omega)$, where $\xi = x_1 - x_2$ and $\eta = y_1 - y_2$ are the spatial separations and $\omega$ is the frequency in rad/sec. The simplest form of the cross-spectral density is the truncated Gaussian white noise pressure uniformly distributed with spatial coordinates x and y

$$S_p(\xi, \eta, f) = \begin{cases} S_0 & if \quad 0 \le f \le f_u \\ 0 & if \quad f < 0 \quad or \quad f > f_u \end{cases} \tag{41}$$

where $S_0$ is constant and $f_u$ is the upper cut-off frequency in Hz. The expression for $S_0$ can be written as [18,22]

$$S_0 = p_0^2 \; 10^{SPL/10} \tag{42}$$

where $p_0$ is the reference pressure, $p_0 = 2.90075 \; 10^{-9}$ psi (20μPa), and sound pressure level (SPL) is expressed in decibels (dB). A typical simulated random load at 90 dB SPL is shown in Figure 2. The band-limited white noise is generated by a Fortran code given in Appendix B that simulates a random pressure using complex numbers with independent random phase angles uniformly distributed between 0 and $2\pi$. The PSD value of the random process is obtained by taking the ensemble average of the Fourier transform of the random load. The PSD value is then compared to the exact one given by Equation (42). The analyses presented are obtained for a cut-off frequency of 1024 Hz for the isotropic and the composite plates. The selected frequency bandwidth is $\Delta\omega = 0$

rad/sec (1 cycle/sec) with the random load prescribed in decibels. For instance, for a uniformly Gaussian random load of 100 dB over a frequency range of 0-1024 Hz corresponds to an overall sound pressure level (OASPL) of 130 dB.

## 3.2 Finite Element and Validation

The nonlinear element equations developed in Equation (17) are general in the sense that they are applicable for beam [28], rectangular [29, 31, and 41], and triangular [30, 44, and 45] plate finite elements. The finite element employed in the present study is the $C^1$-conforming rectangular plate element. The linear stiffness and mass matrices are developed by Bogner-Fox-Schmit (BFS) [46]. The thermal geometrical matrix, thermal load vectors, and nonlinear stiffness matrices are generated using the expressions given in Appendix A. The BFS element has a total of 24 DOF, 16 bending DOF $\{w_b\}$, and 8 in-plane DOF $\{w_m\}$ as shown in Figure 3.

Accurate nonlinear analytical multimode results and test data for panels under acoustic and thermal loads are not available in the literature. Validation of the present nonlinear modal formulation will thus consists of the following two parts: (i) nonlinear free vibrations to assess the accuracy of the left side of Equation (27) with zero damping, and (ii) linear random vibrations to validate the simulated random load $\{\overline{P}\}$ at the right side of Equation (27) with $\Delta T=0$. The accuracy of the nonlinear stiffness matrices in modal coordinates has been verified by Shi et al. [47] for nonlinear free vibration of fundamental and higher modes of plates and beams. The validation of simulated random loads is by comparison of the linear displacements with linear analytical results shown in Table 1. Linear analytical random response is given in Appendix C. The FPK method [48] is an exact solution [49] to the single DOF forced Duffing equation. The present time domain numerical simulation results are also shown in Table 1. The natural frequencies of the lowest seven modes in increasing order are given in Table 2.

**Table 1.** Comparison of RMS $W_{max}/h$ for a Simply-Supported

15×12×0.040 in. Isotropic Plate

| SPL | Linear Analytical | | FE/L/NS | | FPK [48, 49] | FE/NL/NS |
|-----|---------|---------|---------|--------|--------------|----------|
| (dB) | 4 modes | 7 modes | 4 modes | Err.% | 1 mode | 4 modes |
| 90 | 0.2759 | 0.2759 | 0.2760 | 0.0362 | 0.249 | 0.266 |
| 100 | 0.8725 | 0.8725 | 0.8728 | 0.0362 | 0.592 | 0.578 |
| 110 | 2.7590 | 2.7590 | 2.7600 | 0.0362 | 1.187 | 1.432 |
| 120 | 8.7248 | 8.7250 | 8.7281 | 0.0362 | 2.200 | 2.572 |

FE: Finite Element; L: Linear; NL: Non-Linear; NS: Numerical Simulation

**Table 2.** Frequencies (Hz) of a Simply-Supported 15×12×0.040 in. Isotropic Plate

| Mode | (1,1) | (3,1) | (1,3) | (3,3) | (5,1) | (5,3) | (1,5) |
|------|-------|-------|-------|-------|-------|-------|-------|
| Exact | 44.078 | 181.68 | 259.09 | 396.70 | 456.90 | 671.91 | 689.12 |
| FE | 44.082 | 181.70 | 259.10 | 396.75 | 457.02 | 672.06 | 689.29 |

Mesh size is 10x10 in a quarter plate.

## 3.3 Simply Supported Isotropic Plate

A simply supported isotropic plate with immovable in-plane conditions u(0,y)=u(a,y)=v(x,0)=v(x,b)=0 is studied in detail. The plate is of 14 by 10 by 0.04 in. (35.6 by 25.4 by 0.1 cm) and is modeled with a 14 by10 mesh (140 BFS elements) in a quarter plate. The number of structural node DOF $\{W_b\}$ is 560 for the system equations given in Equation (21). The material properties are E=10.5E7 psi (73 GPa), $\nu$=0.3, and $\rho$=2.588x10$^{-4}$ lbf-sec$^2$/in.$^4$ (2763 kg/m$^3$). A proportional damping ratio of $\xi_r\omega_r=\xi_s\omega_s$ with $\xi_1$=0.02 is used. The lowest seven natural frequencies are given in Table 3.

**Table 3.** Frequencies (Hz) of a Simply-Supported 14×10×0.040 in. Isotropic Plate

| Mode | (1,1) | (3,1) | (1,3) | (3,3) | (5,1) | (5,3) | (1,5) |
|-------|--------|--------|--------|--------|--------|--------|--------|
| Exact | 58.116 | 215.19 | 365.98 | 523.05 | 529.33 | 837.19 | 981.70 |
| FE | 58.116 | 215.19 | 365.98 | 523.06 | 529.36 | 837.22 | 981.94 |

The number of modal coordinates to be included in the analyses for converged deflection and strain is studied first. The Root Mean Square (RMS) maximum non-dimensional deflection and the RMS maximum strain versus number of modes at SPL of 120 dB using 1, 2, 4, 6, and 7 modes are shown in Figure 4. The maximum strain is $\varepsilon_y$ at the plate center. The results show that four modes will give converged deflection and strain responses.

Two other studies for accurate and converged response predictions were also performed. They are the finite element mesh sizes and the integration time steps. For a four-mode solution, it was found that a quarter plate model of 14 by 10 mesh size is more than adequate. The time step of integration $\Delta t = 1/8192 = 1.2207 \times 10^{-4}$ sec was first selected, then the time step was cut into one-half with $\Delta t = 1/(2 \times 8192)$ sec. The time histories for the two integration time steps were found to be exactly identical.

Four modes are thus used in the results for the isotropic plate shown in the following: The time histories, PDF and PSD of maximum deflection and strain at SPL =90 and 120 dB and $\Delta T = 0.0$ are shown in Figures 5 and 6, and at SPL=90, 100 and 120 dB and $\Delta T_{cr}/\Delta T = 2.0$ are shown in Figures 7 to 9, respectively. Table 4 gives the statistical moments of the maximum deflection and maximum strain responses. The skewness and kurtosis coefficients are defined as

$$\text{Skewness} = \mu_3/\sigma^3 \tag{43}$$

$$\text{Kurtosis} = (\mu_4/\sigma^4) - 3 \tag{44}$$

where $\mu_k$ and $\sigma$ are the $k^{th}$ central moment and standard deviation, respectively.

**Table 4.** Moments of the $W_{max}/h$ and $\varepsilon_y$ for the 14x10x0.04 in. Isotropic Plate

| SPL dB | $\Delta T_{cr}/\Delta T$ | Rms | Mean in./in. | Variance in.$^2$./in.$^2$. | Skewness in.$^3$./in.$^3$. | Kurtosis in.$^4$./in.$^4$. |
|---|---|---|---|---|---|---|
| | | | $W_{max}/h$ | | | |
| 90 | 0.0 | 0.1608 | $1.241 \times 10^{-4}$ | 0.0258 | 0.0242 | -0.4320 |
| 120 | 0.0 | 1.4039 | $-2.628 \times 10^{-3}$ | 1.9714 | 0.00634 | -0.8613 |
| 90 | 2.0 | 0.8239 | -0.8163 | 0.0124 | 2.0074 | 9.4296 |
| 100 | 2.0 | 0.7470 | -0.1052 | 0.5470 | -0.2480 | -1.3823 |
| 120 | 2.0 | 1.5770 | $1.999 \times 10^{-3}$ | 2.4873 | 0.00272 | -0.7367 |
| | | | **Strain** | | | |
| | | | $\mu$in./in. | $\mu$in.$^2$./in.$^2$. | in.$^3$./in.$^3$. | in.$^4$./in.$^4$. |
| 90 | 0.0 | $1.324 \times 10^{-5}$ | -0.0176 | 0.000175 | -0.0432 | -0.4050 |
| 120 | 0.0 | $1.167 \times 10^{-4}$ | 22.268 | 0.01312 | 0.5744 | 0.4317 |
| 90 | 2.0 | $4.035 \times 10^{-5}$ | -39.094 | 0.000333 | 0.22477 | 0.1467 |
| 100 | 2.0 | $6.612 \times 10^{-5}$ | 21.692 | 0.003902 | 0.26784 | -1.2727 |
| 120 | 2.0 | $19.02 \times 10^{-5}$ | 72.950 | 0.031171 | -0.5501 | -0.1875 |

At the low 90 dB SPL, the plate behaviors basically small deflection ($W_{max}/h$=0.1608) random vibration dominated by the fundamental (1,1) mode as shown in the PSD plots of Figure 5. The probabilities for deflection and strain are both closely to Gaussian. The time history at the high 120 dB SPL in Figure 6 is clearly a large deflection ($W_{max}/h > 1.0$) nonlinear random. This is demonstrated by the peaks in PSD plots that they are broadening and shifting to the higher frequency, and by the presence of a non-zero mean in-plane strain shown in the strain plots. The large deviation from the Gaussian is shown by the strain PDF and the larger kurtosis value for deflection and skewness value for strain in Table 4.

At combined acoustic and thermal loads, the panel responses show the three distinct motions of the following (i) small deflection random vibration about one of the two thermally buckled equilibrium positions in Figure 7, (ii) snap-through or oil-canning

phenomenon between the two thermally buckled positions in Figure 8, and (iii) large amplitude nonlinear random vibration covering both thermally buckled positions shown in Figure 9.

At low 90 dB and $\Delta T/\Delta T_{cr}=2.0$, the time histories in Figure 7 clearly show the linear random responses about one of the thermally buckled positions of $(W_{max}/h)_{\Delta T}= -0.8163$. The deflection PSD plot shows the domination of the fundamental mode, and the strain PSD plot shows the equally contribution from the third mode. Also, note that the general increase of the panel vibration frequencies, e.g., from 58 Hz (Figure 5 at $\Delta T=0$) to 86 Hz (Figure 7 at $\Delta T/\Delta T_{cr}=2.0$) for the fundamental mode. As the SPL increased to 100 dB, the time histories in Figure 8 show that snap-through motions and the deflection PDF is non-Gaussian. This confirms clearly the drawback in using EL approach with the Gaussian response assumption. At high SPL of 120 dB in Figure 9, the large deflection RMS $W_{max}/h$ is 1.5770 which covers both buckled positions of $(W_{max}/h)_{\Delta T}=\pm0.8163$. Nonlinearities are further observed by the broadening and shifting of the peaks in the PSD plots.

## 3.4 Clamped Composite Plate

Nonlinear response of a composite plate subjected to combined acoustic and thermal loads can be determined using the present modal formulation. Three types of panel behavior are as follows: (i) small deflection random vibration about one of the two thermally buckled equilibrium positions, (ii) snap-through or oil canning phenomenon between the two buckled positions, and (iii) large nonlinear random vibration covering both thermally buckled positions, can be predicted. As shown in the second example, a clamped rectangular Graphite-Epoxy plate of eight layers $[0/45/-45/90]_s$ is investigated. The plate is of 15 by 12 by 0.048 in. (38.1 by 30.5 by 0.12 cm) and the material properties are the following: $E_1=22.5$ Msi (155 GPa), $E_2=1.17$ (8.07), $G_{12}=0.66$ (4.55), $\rho=0.1468\times10^{-3}$ lb-sec$^2$/in.$^4$ (1550 kg/m$^3$), $v_{12}=0.22$, $\alpha_1=-0.04\times10^{-6}/^\circ$F ($-0.07\times10^{-6}/^\circ$C), and $\alpha_2=16.7\times10^{-6}$ ($30.1\times10^{-6}$). A proportional damping ratio with $\xi_1=0.01$ is used. The in-plane edges are immovable and the plate is modeled with a 6 by 6 mesh quarter plate.

22

The number of system equations in structure node DOF $\{W_b\}$ is 121. The system equations are reduced to the modal coordinates using the lowest four symmetric modes.

The maximum deflection and the maximum strain response time histories, PDF and PSD at $\Delta T/\Delta T_{cr}=2.0$ and SPL=90, 100, and 120 dB, are shown in Figures 10 to 12, respectively. The time histories, PDF and PSD plots clearly show the three distinctive motions of linear vibration about one of the buckled positions at low 90 dB SPL, oil-canning jump behavior at moderate 100 dB, and large deflection nonlinear random vibration at high SPL of 120 dB. It is also interesting to note that the maximum thermal deflection $(W_{max}/h)_{\Delta T}$ of the plate at $\Delta T/\Delta T_{cr}=2.0$ can be also obtained from the deflection time histories in Figures 10 and 11. The maximum thermal deflection from the time history plots is $W_{max}/h=\pm1.1446$ at $\Delta T/\Delta T_{cr}=2.0$, and the thermal postbuckling analyses are $\Delta T_{cr}=36.52$ °F and $(W_{max}/h)=\pm1.134$ from reference [50]. The deflection PDF plots shown in Figures 10 to 12 demonstrate the large deviation from Gaussian distribution. The statistical moments for the maximum deflection and maximum strain response are presented in Table 5. The nonlinearities of the response are indicated also by the PSD in Figures 11 and 12 and the large values of kurtosis.

**Table 5.** Moments of the $W_{max}/h$ and $\varepsilon_y$ for the

Clamped $[0/45/-45/90]$s Plate at $\Delta T/\Delta T_{cr}=2.0$

| SPL dB | Rms | mean in./in. | variance $in^2./in^2.$ | skewness $in^3./in^3.$ | kurtosis $in^4./in^4.$ |
|---|---|---|---|---|---|
| | | | $W_{max}/h$ | | |
| 90 | 1.1487 | -1.1446 | 0.0103 | 2.4667 | 18.387 |
| 100 | 1.0683 | 0.4701 | 0.9388 | -0.8812 | -0.8872 |
| 120 | 1.3312 | 0.0064 | 1.7777 | -0.0125 | -1.1648 |
| | | | Strain | | |
| | | $\mu in./in.$ | $\mu in^2./in^2.$ | $in^3./in^3.$ | $in^4./in^4.$ |
| 90 | $6.107 \times 10^{-5}$ | 5.0390 | 0.003705 | -0.12307 | -0.28389 |
| 100 | $1.289 \times 10^{-4}$ | 128.94 | 0.148640 | -0.02496 | -0.26830 |
| 120 | $3.699 \times 10^{-4}$ | 369.88 | 1.048371 | -0.31806 | -0.10084 |
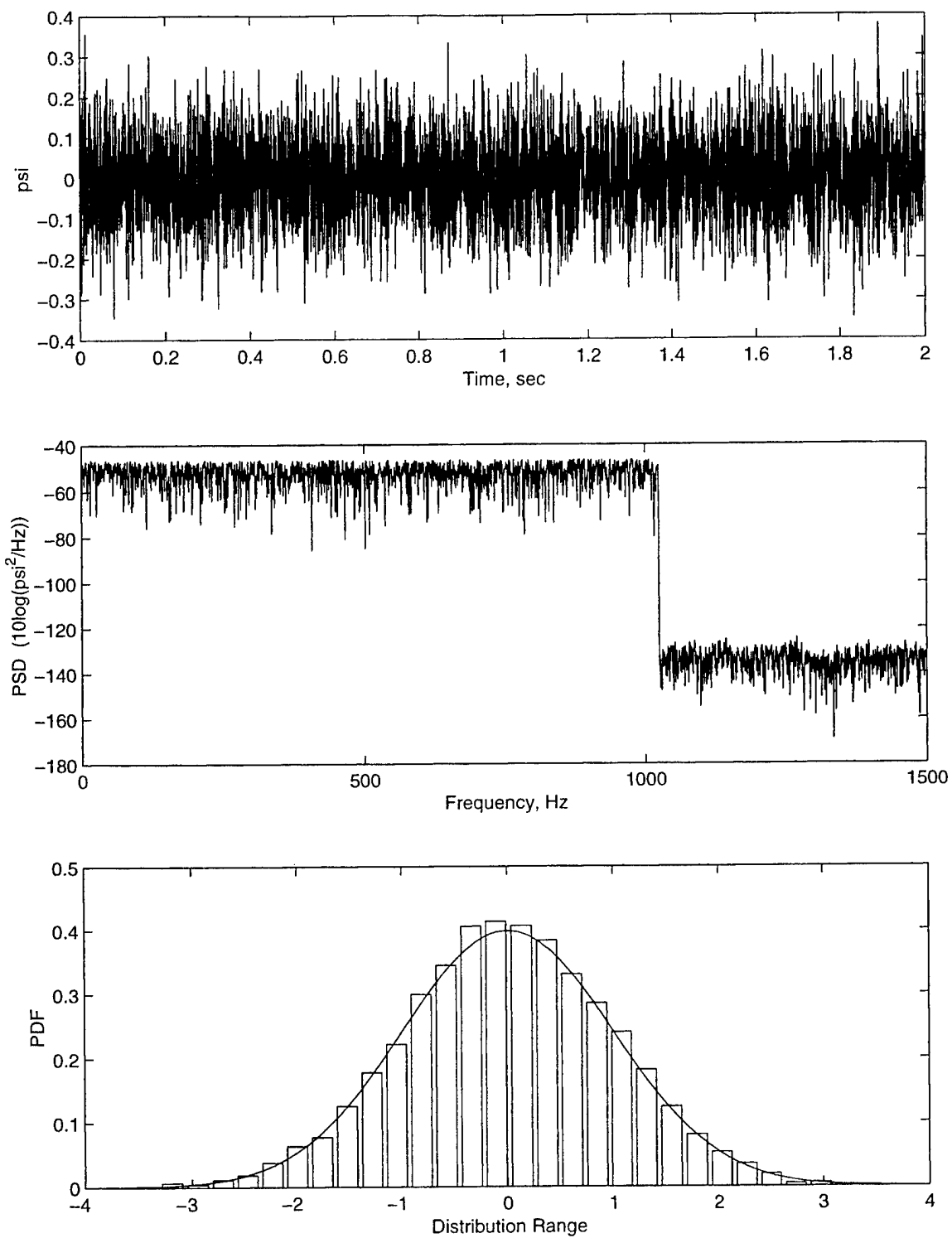
**Figure 2.** Random Noise Generation
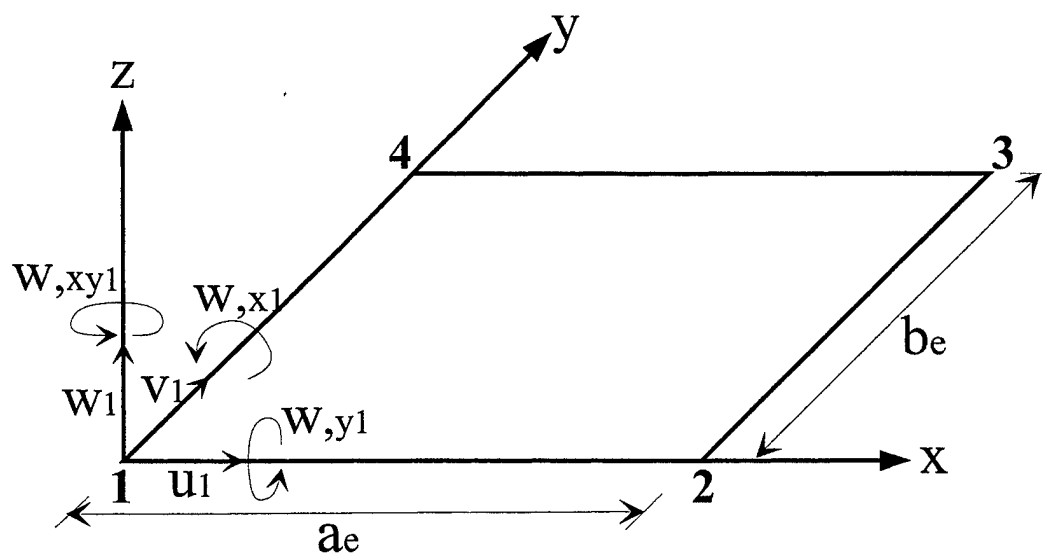
**Figure 3.** Nodal Degrees of Freedom of a BFS C1-Conforming
Rectangular Plate Element
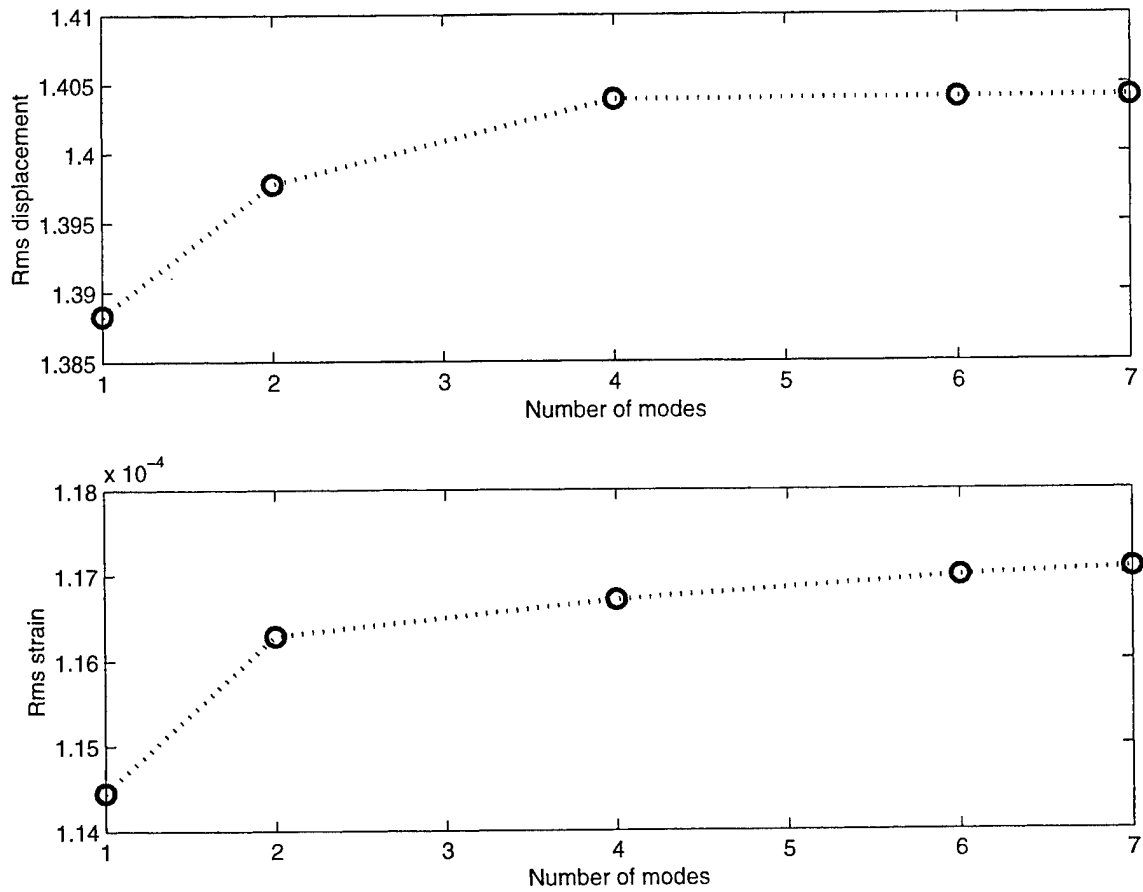
**Figure 4.** Convergence of RMS Maximum Deflection and

Strain for a Simply Supported Isotropic Plate at 120 dB SPL
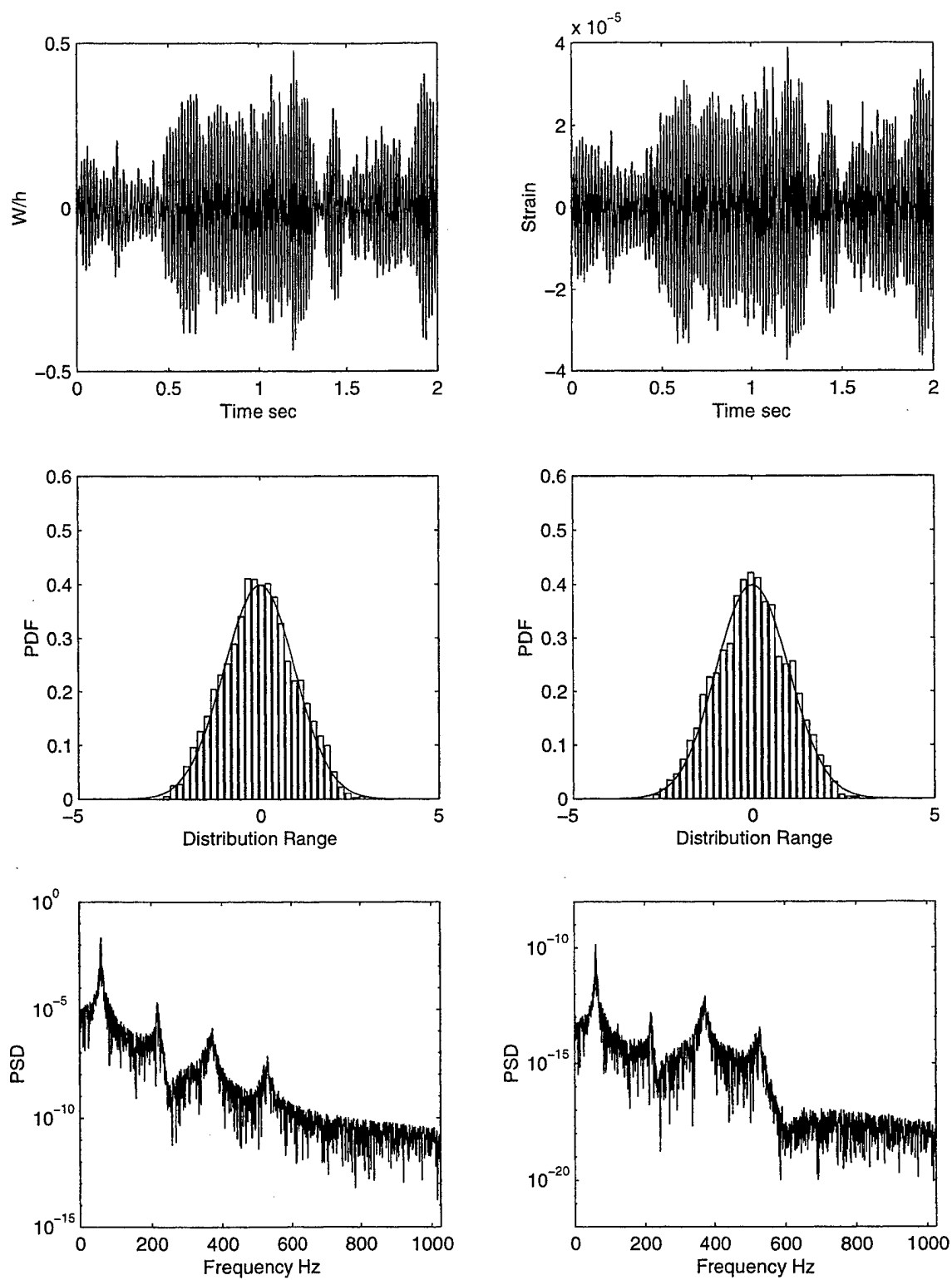
**Figure 5.** Response of a Simply Supported Isotropic Plate at 90 dB and $\Delta T$=0.0

27
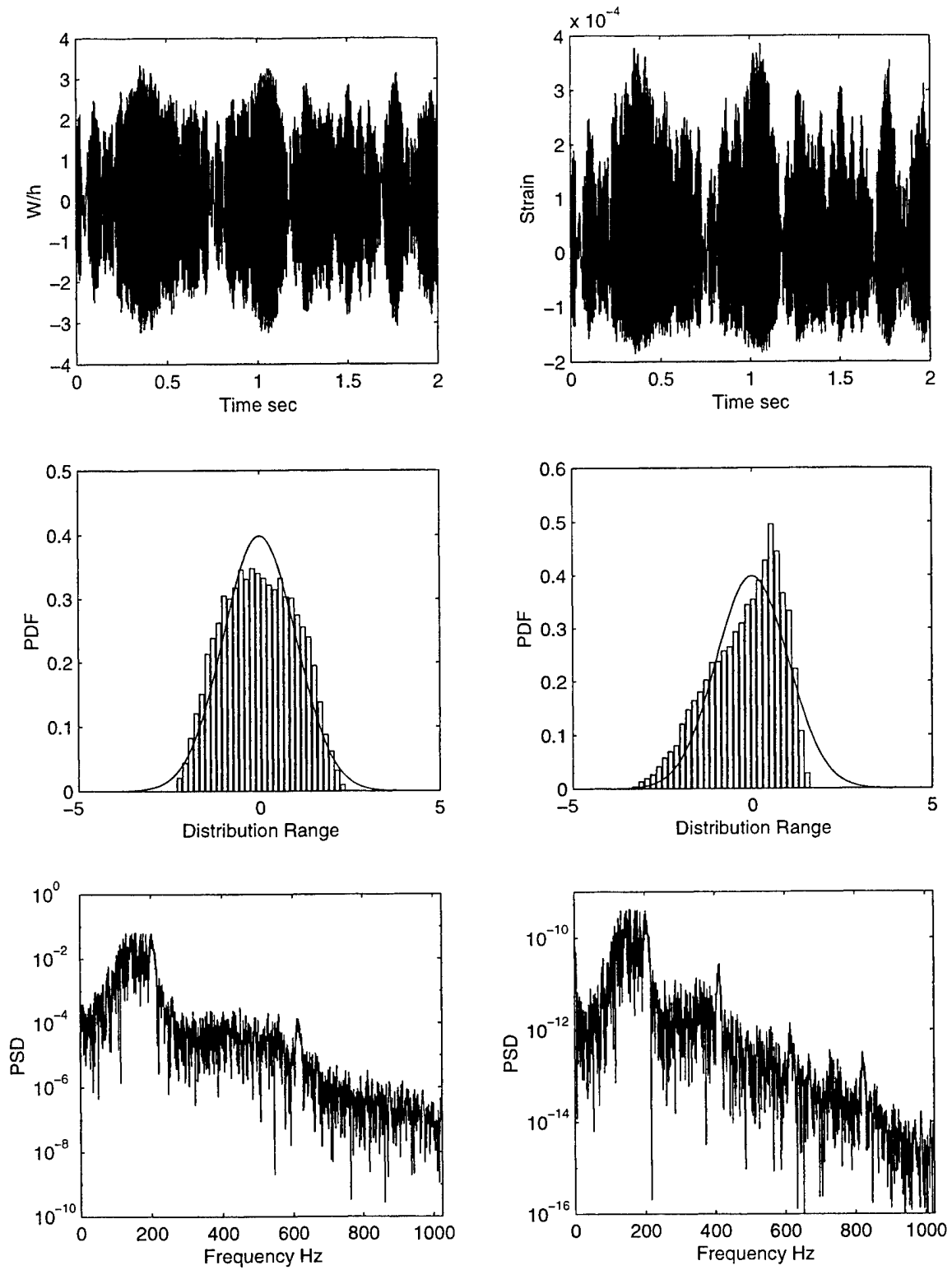
**Figure 6.** Response of a Simply Supported Isotropic Plate at 120 dB and ΔT=0.0
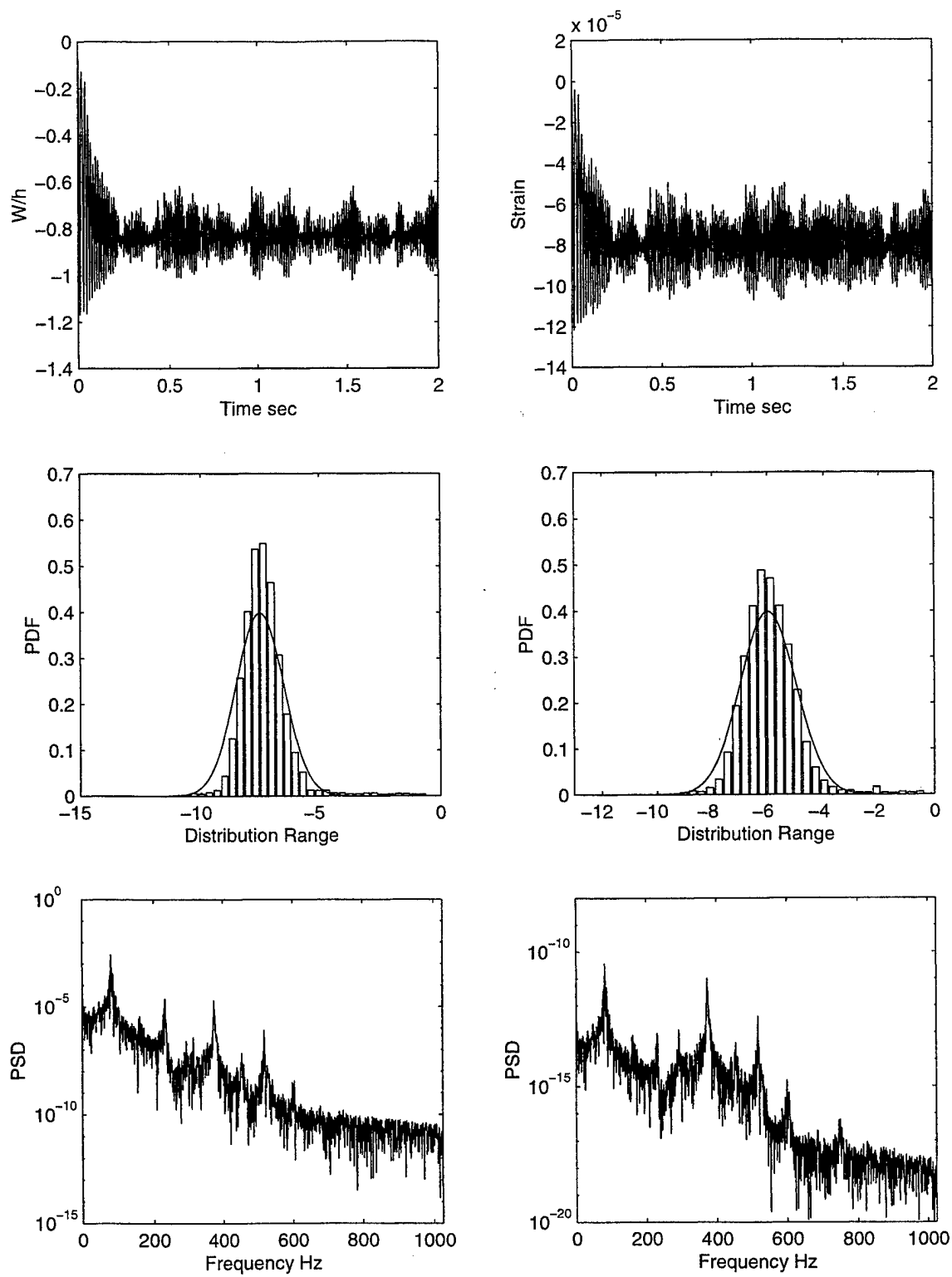
**Figure 7.** Response of a Simply Supported Isotropic Plate at 90 dB and $\Delta T /\Delta T_{cr}$=2.0

29
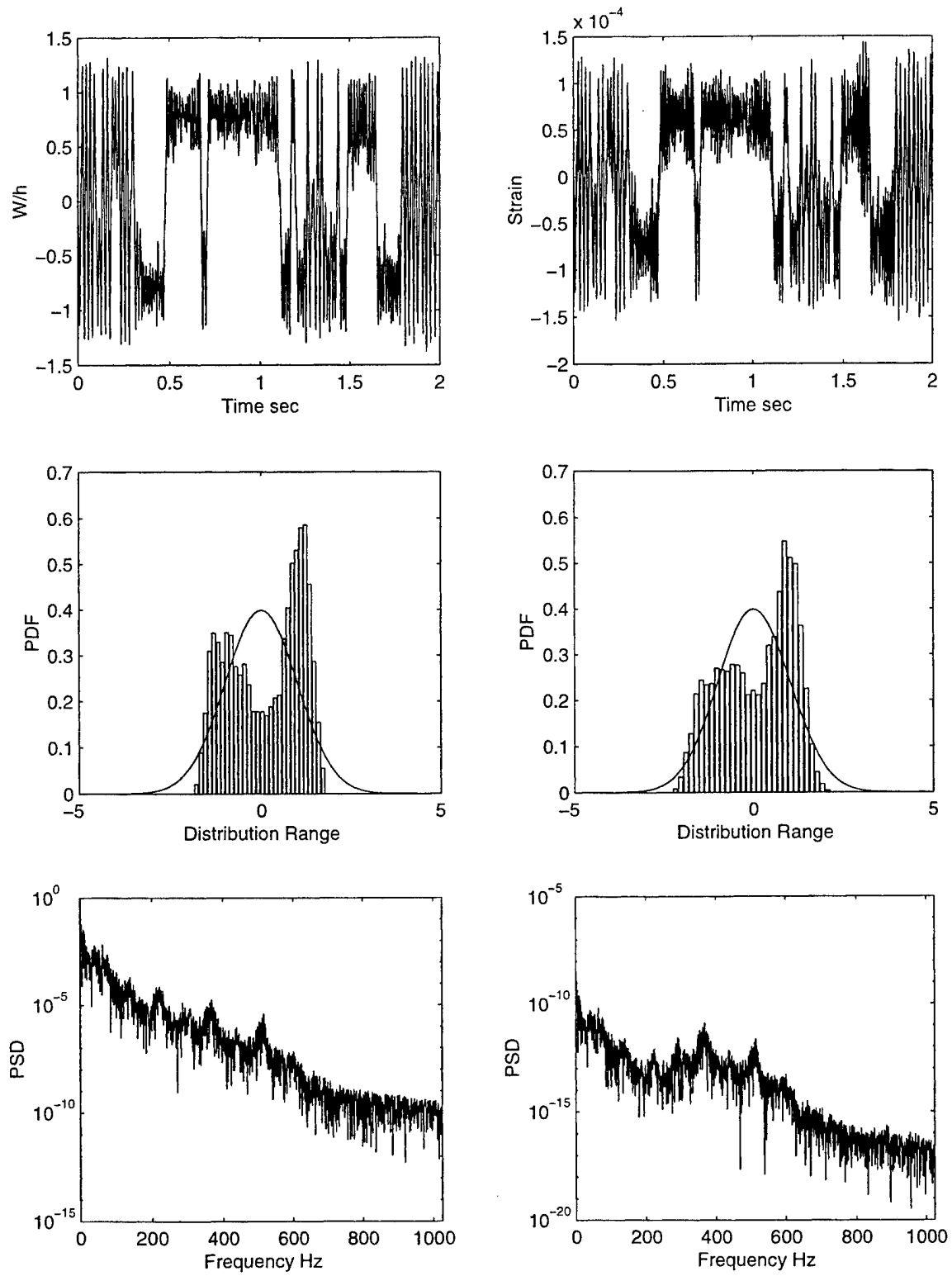
**Figure 8.** Response of a Simply Supported Isotropic Plate at 100 dB and $\Delta T / \Delta T_{cr} = 2.0$
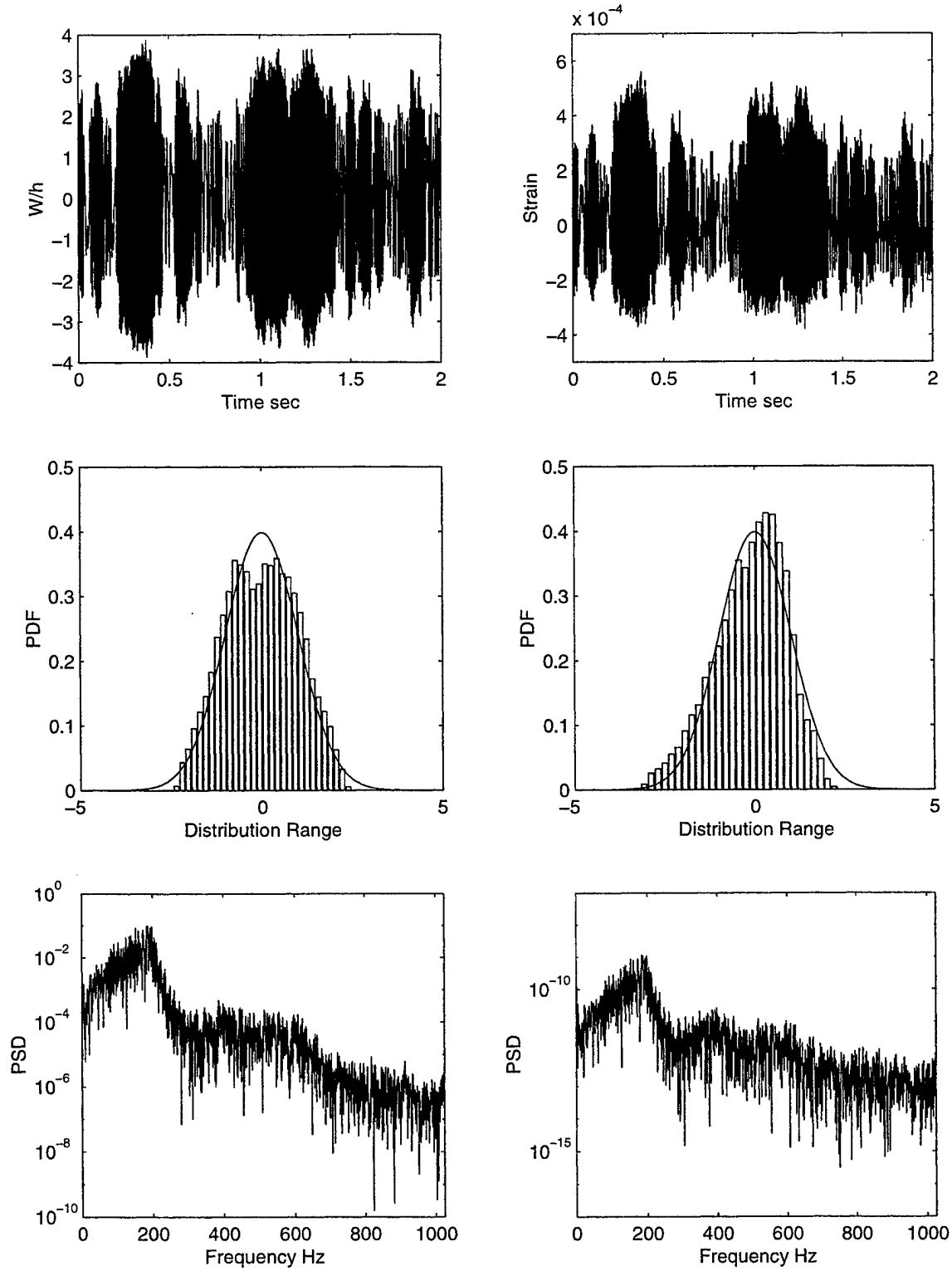
**Figure 9.** Response of a Simply Supported Isotropic Plate at 120 dB and $\Delta T / \Delta T_{cr}=2.0$
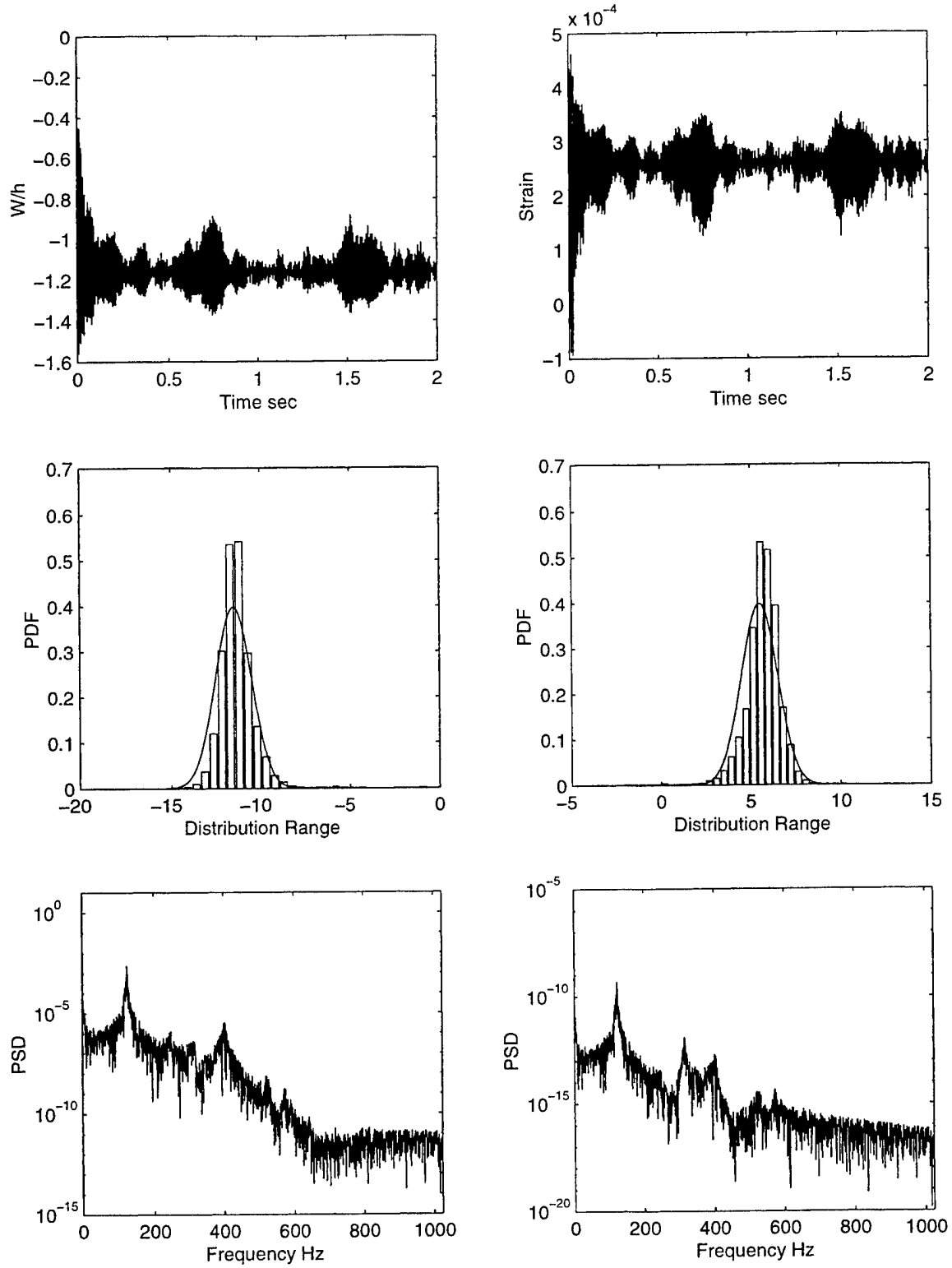
**Figure 10.** Response of a [0/45/-45/90]$_s$ Composite Plate

at SPL=90 dB and $\Delta T/\Delta T_{cr}$=2.0
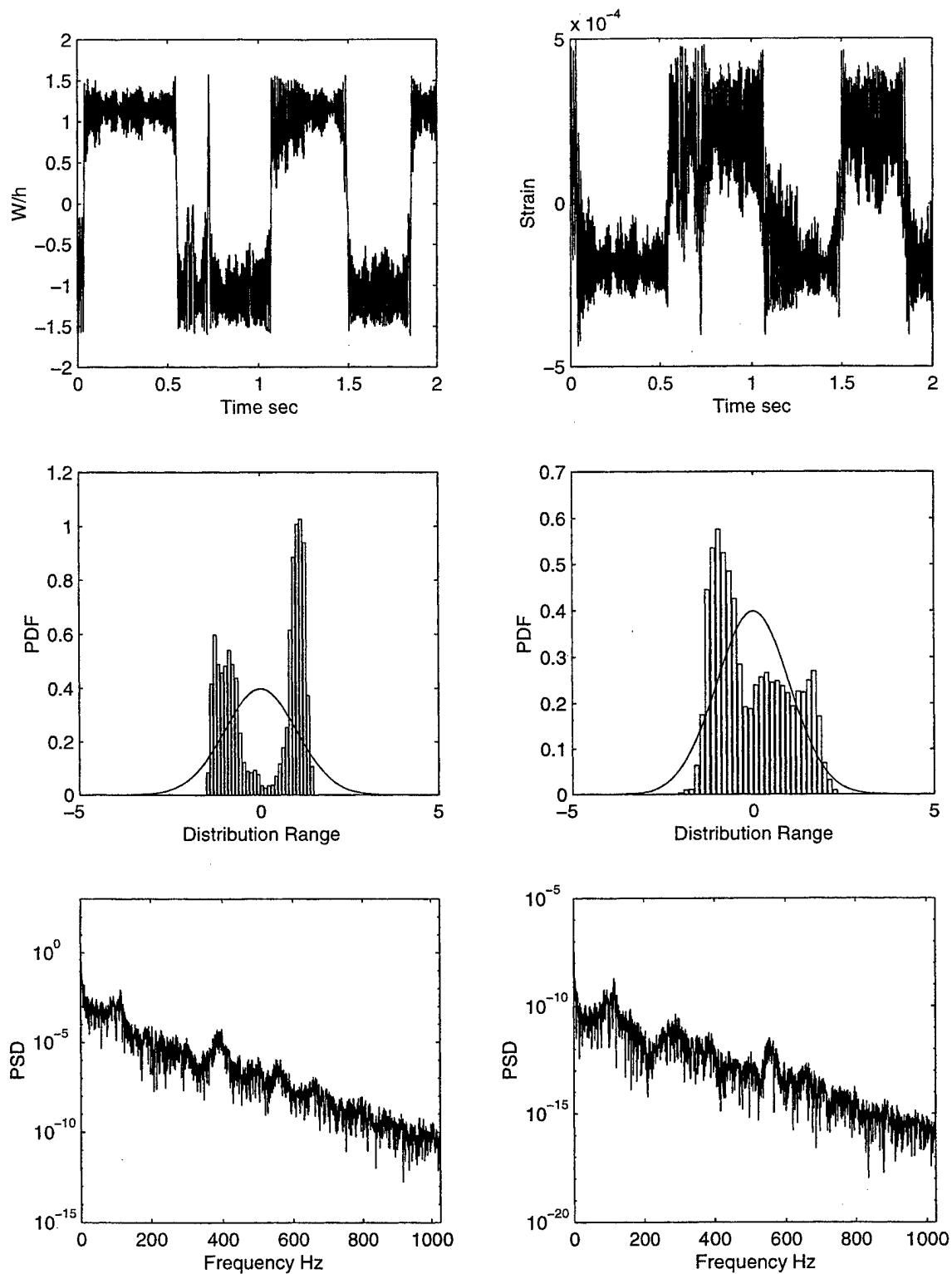
**Figure 11.** Response of a [0/45/-45/90]$_s$ Composite Plate

at SPL=100 dB and $\Delta T/\Delta T_{cr}$=2.0
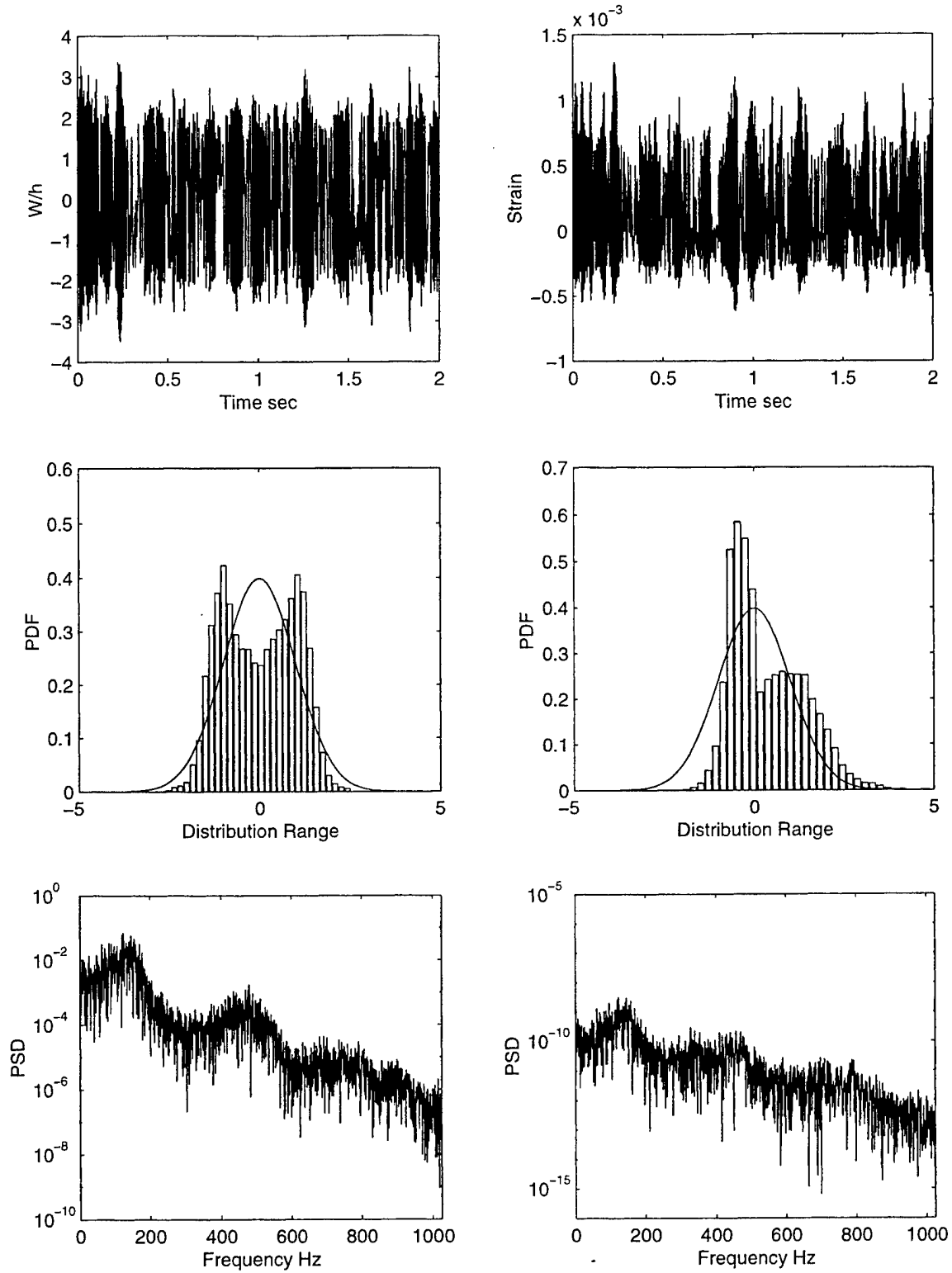
**Figure 12.** Response of a [0/45/-45/90]$_s$ Composite Plate

at SPL=120 dB and $\Delta T/\Delta T_{cr}$=2.0

# 4. Conclusion

A finite element time domain modal formulation is presented for the prediction of nonlinear random response of composite panels subjected to acoustic pressure at elevated temperature. The modal formulation is computationally efficient that the following occur: (i) the number of modal equations is small, (ii) the nonlinear modal stiffness matrices are constant matrices, and (iii) the time step of integration could be reasonably large. It is demonstrated that the following three types of panel motions can be predicted: (i) linear random vibration about one of the buckled equilibrium position, (ii) snap-through motions between the two buckled positions, and (iii) nonlinear random response over both buckled positions. Results of deflection PDF at the high SPL also show that the assumption of Gaussian distribution by the equivalent linearization technique is inappropriate.

# References

1. Crandall, S. H. and Zhu, W. Q., "Random Vibration: A Survey of Recent Developments," Journal Applied Mechanics, Transactions of the ASME 50th Anniversary, Vol. 50, 1983, pp. 953-962.

2. To, C. W. S., "The Response of Nonlinear Structures to Random Excitation," Shock and Vibration Digest, Vol. 16, April 1984, pp. 13-33.

3. Roberts, J.B., "Techniques for Nonlinear Random Vibration Problems," Shock and Vibration Digest, Vol. 16, September 1984, pp. 3-14.

4. Spanos, P. D. and Lutes, L. D., "A Primer of Random Vibration Techniques in Structural Engineering," Shock and Vibration Digest, Vol. 18, April 1986, pp. 3-9.

5. Caughey, T. K., "Derivation and Application of the FPK Equation to Discrete Nonlinear Dynamic Systems to White Random Excitation," Journal Acoustic Society of America, Vol. 35, November 1963, pp. 1683-1692.

6. Roberts, J. B., "Response of Nonlinear Mechanical Systems to Random Excitation, Part I: Markov Methods," Shock and Vibration Digest, Vol. 13, April 1981, pp. 17-28.

7. Caughey, T. K. and Ma, F., " The Exact Steady-State Solution of a Class of Nonlinear Stochastic Systems," International Journal Nonlinear Mechanics, Vol. 17, No. 3, 1982, pp. 137-142.

8. Lyon, R. H., "Response of a Nonlinear String to Random Excitation," Journal Acoustic Society of America, Vol. 32, No. 8, 1960, pp. 953-960.

9. Crandall, S. H., "Perturbation Techniques for Random Vibration of Nonlinear Systems," Journal Acoustic Society of America, Vol. 35, No. 11, 1963, pp. 1700-1705.

10. Iwan, W. D. and Yang, M. I., "Application of Statistical Linearization Techniques to Nonlinear Multi-Degree of Freedom Systems," Journal of Applied Mechanics, Vol. 39, June 1972, pp. 545-550.

11. Booton, R. C., "The Analysis of Nonlinear Control Systems with Random Inputs," Circuit Theory, IRE Transactions, Vol. 1, 1954, pp. 32-34.

12. Caughey, T. K., "Equivalent Linearization Techniques," Journal Acoustic Society of America, Vol. 35, No. 11, 1963, pp. 1706-1711.

13. Atalik, T. S. and Utku, S., "Stochastic Linearization of Multi-Degree-of-Freedom Nonlinear Systems," Earthquake Engineering and Structural Dynamics, Vol. 4, July-August 1976, pp. 411-420.

14. Roberts, J. B. and Spanos, P. D., "Random Vibration of Statistical Linearization," John Wiley & Sons, NY, 1990.

15. Shinozuka, M., "Monte Carlo Solution of Structural Dynamics," International Journal of Computers and Structures, Vol. 2., 1972, pp. 855-874.

16. Shinozuka, M. and Wen, Y. K., "Monte Carlo Solution of Nonlinear Vibrations," AIAA Journal, Vol. 10, No. 1, 1972, pp. 37-40.

17. Shinozuka, M. and Jan, D. M., "Digital Simulation of Random Processes and Its Applications," Journal of Sound and Vibration, Vol. 25, 1972, pp. 111-128.

18. Rudder, F. F. and Plumblee, H. E., "Sonic Fatigue Design Guide for Military Aircraft," AFFDL-TR-74-112, Wright-Patterson AFB, OH, 1975.

19. Holehouse, I., "Sonic Fatigue Design Guide Techniques for Advanced Composite Structures," Ph. D. Dissertation, University of Southampton, UK, 1984.

20. Vaicaitis, R., "Recent Advances of Time Domain Approach for Nonlinear Response and Sonic Fatigue," Proceedings 4th International Conference on Structural Dynamics, ISVR, University of Southampton, UK, July 1991, pp. 84-103.

21. Vaicaitis, R., "Time Domain Approach for Nonlinear Response and Sonic Fatigue of NASP Thermal Protection Systems," Proceedings of 32nd Structures, Structural Dynamics, and Materials Conference, Baltimore, MD, April 1991, pp. 2685-2708.

22. Arnold, R. R. and Vaicaitis, R., "Nonlinear Response and Fatigue of Surface Panels by the Time Domain Monte Carlo Approach," WRDC-TR-90-3081, Wright-Patterson AFB, OH, 1990.

23. Vaicaitis, R. and Kavallieratos, P. A., "Nonlinear Response of Composite Panels to Random Excitation," Proceedings 34th Structures Structural Dynamics, and Materials Conference, La Jolla, CA, April 1993, pp. 1041-1049.

24. Lee, J., "Large-Amplitude Plate Vibration in an Elevated Thermal Environment," Applied Mechanics Reviews, Vol. 46, Part 2, 1993, pp. S242-254.

25. Lee, J., "Random Vibration of Thermally Buckled Plates: I. Zero Temperature Gradient Across the Plate Thickness," AIAA Progress Series in Aeronautics and Astronautics, E.A. Thorton. Editor, 1995.

26. Lee, J., "Improving the Equivalent Linearization Technique for Stochastic Duffing Oscillators," Journal of Sound and Vibration, Vol. 186(5), 1995, pp. 846-855.

27. Crandall, S. H., "Non-Gaussian Closure for Random Vibration of Non-Linear Oscillators," International Journal Non-Linear Mechanics, Vol. 15, 1980, pp. 303-313.

28. Locke, J. E, and Mei, C., "A Finite Element Formulation for the Large Deflection Random Response of Thermally Buckled Beams," AIAA Journal, Vol. 28, 1990, pp. 2125-2131.

29. Locke, J. E., "A Finite Element Formulation for the Large Deflection Random Response of Thermally Buckled Structures," Ph.D. Dissertation, Old Dominion University, Norfolk, VA, 1988.

30. Mei, C. and Chen, R. R., "Finite Element Nonlinear Random Response of Composite Panels of Arbitrary Shape to Acoustic and Thermal Loads Applied Simultaneously," WL-TR-97-3085, Wright-Patterson AFB, OH, 1997.

31. Shi, Y. and Mei, C., "Coexisting Thermal Postbuckling of Composite Plates with Initial Imperfections Using Finite Element Modal Methods," Proceedings 37th Structures, Structural Dynamics, and Materials Conference, Salt Lake City, UT, April 1996, pp. 1355-1362.

32. Ng, C. F. and Clevenson. S. A., "High-Intensity Acoustic Tests of a Thermally Stresses Plate," Journal of Aircraft, Vol. 28, No. 4, 1991, pp. 275-281.

33. Istenes, R. R., Rizzi, S. A. and Wolfe, H. F., "Experimental Nonlinear Random Vibration Results of Thermally Buckled Composite Panels," Proceedings of 36th Structures, Structural Dynamics, and Materials Conference, New Orleans, LA, April 1995, pp. 1559-1568.

34. Murphy, K. D., "Theoretical and Experimental Studies in Nonlinear Dynamics and Stability of Elastic Structures," Ph.D. Dissertation, Duke University, Durham, NC, 1994.

35. Murphy, K. D., Virgin, L. N. and Rizzi, S.A., "Experimental Snap-Through Boundaries for Acoustic Excited Thermally Buckled Plates," Experimental Mechanics, Vol. 36, No. 4, 1996, pp. 312-317.

36. Mei, C. and Wolfe, H. F., "On Large Deflection Analysis in Acoustic Fatigue Design," Random Vibration: Status and Recent Development, The S.H. Crandall Festschrift, Elsevier Science, 1986, pp. 279-302.

37. Benaroya, H. and Rebak, M., "Finite Element Methods in Probabilistic Structural Analysis: A Selective Review," Applied Mechanics Reviews, Vol. 41, No. 5, 1988, pp. 201-213.

38. Clarkson, B. L., "Review of Sonic Fatigue Technology," NASA CR-4587, 1994.

39. Wolfe, H. F., Shroger, C.A., Brown, D.L. and Simmons, L.W., "An Experimental Investigation of Nonlinear Behavior of Beams and Plates Excited to High Levels of Dynamic Response," WL-TR-96-3057, Wright-Patterson AFB, OH, 1995.

40. Green, P. D. and Killey, A., "Time Domain Dynamic Finite Element Modeling in Acoustic Fatigue Design," Proceedings 6th International Conference on Structural Dynamics, ISVR, 1997, pp. 1007-1026.

41. Robinson, J. H., "Finite Element Formulation and Numerical Simulation of the Large Deflection Random Vibration of Laminated Composite Plates," MS Thesis, Old Dominion University, 1990.

42. Barlow, J., "Optimal Stress Locations in Finite Element Models," International Journal for Numerical Methods in Engineering, Vol. 10, 1976, pp. 243-251.

43. Cook, R. D., Malkus, D. S. and Plesha, M. E., "Concepts and Applications of Finite Element Analysis," 3rd Edition, John Wiley, New York, 1989, p. 189.

44. Xue, D. Y., "A Finite Element Frequency Domain Solution of Nonlinear Panel Flutter with Temperature Effects and Fatigue Life Analysis," Ph.D. Dissertation, Old Dominion University, Norfolk, VA, 1991.

45. Xue, D. Y. and Mei, C., "Finite Element Nonlinear Panel Flutter with Arbitrary Temperatures in Supersonic Flow," AIAA Journal, Vol. 31, 1993, pp. 154-162.

46. Bogner, F. K., Fox, R. L. and Schmit, L. A., "The Generation of Inter-Element Compatible Stiffness and Mass Matrices by the Use of Interpolation Formulas," AFFDL-TR-66-80, Wright-Patterson AFB, OH, 1996, pp. 396-443.

47. Shi, Y., Lee, R. and Mei, C., "A Finite Element Multimode Method to Nonlinear Free Vibrations of Composite Plates," AIAA Journal, 1997, Vol. 35, pp. 159-166.

48. Bolotin, V.V., "Random Vibration of Elastic Systems," Martinus Nijhoff Publishers, 1984, pp. 290-292.

49. Chiang, C.K., "A Finite Element Large Deflection Multi-Mode Random Response Analysis of Complex Panels with Initial Stresses Subjected to Acoustic Loading," Ph.D. Dissertation, Old Dominion University, Norfolk, VA, 1988.

50. Mei, C., Duan, B., Zhang, Z. and Wolfe, H.F. "Large Thermal Deflections of Composite Plates with Temperature Dependent Properties," AFRL-VA-WP-TR-1999-3036, Wright-Patterson AFB, OH, 1999.

51. Lutes, D.L. and Sarkani, S., "Stochastic Analysis of Structural and Mechanical Vibrations," Prentice-Hall, New Jersey 07458, 1997.

# Appendix A

## Element Matrices and Load Vectors

A1. Linear Stiffness Matrices

$$[k_b] = \int_A [B_b]^T [D][B_b] dA \tag{A1}$$

$$[k_B] = [k_B]^T = \int_A [B_m]^T [B][B_b] dA \tag{A2}$$

$$[k_m] = \int_A [B_m]^T [A][B_m] dA \tag{A3}$$

$$[k_{N\Delta T}] = \int_A [B_\theta]^T [N_{\Delta T}][B_\theta] dA \tag{A4}$$

A2. First-Order and Second-Order Stiffness Matrices

$$[k_{1Nm}] = \frac{1}{2} \int_A [B_\theta]^T [N_m][B_\theta] dA \tag{A5}$$

$$[k_{1mb}] = [k_{1bm}]^T = \frac{1}{2} \int_A [B_m]^T [A][\theta][B_\theta] dA \tag{A6}$$

$$[k_{1NB}] = \frac{1}{2} \int_A \left( [B_\theta]^T [\theta]^T [B][B_b] + [B_\theta]^T [N_B][B_\theta] + [B_b]^T [B][\theta][B_\theta] \right) dA \tag{A7}$$

$$[k_{2b}] = \frac{1}{2} \int_A [B_\theta]^T [\theta]^T [A][\theta][B_\theta] dA \tag{A8}$$

A3. Load Vectors

$$\{p_{b\Delta T}\} = \int_A [B_b]^T \{M_{\Delta T}\} dA \tag{A9}$$

$$\{p_{\Delta Tm}\} = \int_A [B_m]^T \{N_{\Delta T}\} dA \tag{A10}$$

$$\{p_b(t)\} = \int_A \{H_w\} p(t) dA \tag{A11}$$

A4. Mass Matrices

$$[m_b] = \rho h \int_A \{H_w\} \lfloor H_w \rfloor dA \tag{A12}$$

$$[m_m] = \int_A \rho h \left( \{H_u\} \lfloor H_u \rfloor + \{H_v\} \lfloor H_v \rfloor \right) dA \tag{A13}$$

41

# Appendix B

**Fortran Code for Gaussian-Stationary Random Load Generation.**

```
C****************************************************************
C
C                         SIMLOAD
C
C****************************************************************
C   N              --NO. OF INTERVALS IN THE SPECTRUM
C                    N  SHOULD BE AN INTEGER POWER OF TWO
C   NPT            --NO.OF POINTS FOR THE TIME SERIES
C                    NPT SHOULD BE INTEGER POWER OF TWO. NPT>N
C   ISEED          --RANDOM NUMBER SEED
C   TTOTAL  = N/FMAX      TTOTAL IS THE TOTAL INTEGRATION TIME
C   DT = N/(NPT*FMAX)  DT IS THE INTEGRATION TIME STEP SIZE
C------------------------------------------------------------
C****************************************************************
C INSTRUCTIONS FOR SETTING THE DATA
C ------------------------------------------------------------
C 1- TAKE HIGHEST FREQUENCY, FMAX
C 2- MINIMUM TIME STEP IS STEP_MIN=1/(2.5xFMAX)
C 3- N=FMAX x 2
C 4- PICK UP TOTAL RUNNING TIME (1 SEC, 2 SEC ...) T_total=N/FMAX
C 5- SELECT NPT TO SATISFY 2-
C                               N
C                   STEP=----------------
C                           NPT x FMAX
C
C****************************************************************
      PROGRAM SIMLOAD
      IMPLICIT REAL*8 (A-H,O-Z)
C     COMMON /XFER/ISTEP,DSTEP,DT,Y(16384)
C     COMMON /XFER/DT,Y(16384)
C     REAL*8 DT,Y(2)
      DIMENSION X(16384),Y(16384),SP(2048),W(2048),RAND(16384)
      COMPLEX X,ZIMAG
      OPEN (1,file='d:\research\load_st\pressure.dat')
      OPEN (2,file='d:\research\load_st\npt.dat')
      OPEN (3,file='d:\research\load_st\fmax.dat')
      OPEN (4,file='d:\research\load_st\n.dat')
      DATA FMAX/1024./
      DATA N,NPT /2048,16384/
C****************************************************************
```

```
C                          INITIALIZE VARIABLES
C*******************************************************************
C     SPL=120
C     SPP = 8.41438*10**(-18.+SPL/10.)
      PI = 3.1415926
      PI2 = PI*2.0
      NP1 = N+1
      ZIMAG = CMPLX(0.0,1.0)
      SPPW = SPP/PI2
      WU = FMAX*PI2
      DW = WU/FLOAT(N)
      DO 119 I=1,NP1
        SP(I) = SPPW
        W(I) = (I-1)*DW
119   CONTINUE
      AREA = SPP*FMAX
      SQ2DW = DSQRT(2.0*DW)
      TTOTAL=PI2/DW
      DT=TTOTAL/FLOAT(NPT)
C*******************************************************************
C  SET X(1)=0. IN ORDER TO OBTAIN NEW MEAN ZERO TIME SERIES
C*******************************************************************
      X(1)=CMPLX(0.0,0.0)
      DO 50 I=N+1,NPT
           X(I)=CMPLX(0.0,0.0)
50    CONTINUE
C*******************************************************************
C     GENERATE RANDOM PHASE ANGLES UNIFORMLY DISTRIBUTED
BETWEEN  ZERO AND 2.*PI
C*******************************************************************
      ISEED=12357
         DO 51 I=1,N
51    RAND(I)=RAN(ISEED)
      DO 60 I=2,N+1
        PHI=RAND(I-1)*PI2
        P1=SQ2DW*DSQRT(SP(I))
        X(I)=P1*CDEXP(-ZIMAG*PHI)
60    CONTINUE
C*******************************************************************
C                    PERFORM FORWARD TRANSFORM
C*******************************************************************
      CALL FFT(X,NPT,1)
C*******************************************************************
C                         GET REAL PART
C*******************************************************************
      DO 70 I=1,NPT
```

```fortran
         Y(I)=REAL(X(I))
70    CONTINUE
         WRITE(1,FMT=100) Y
100   FORMAT (f18.8)
         WRITE (2,*) NPT
         WRITE (3,*) FMAX
         WRITE (4,*) N,DT,SPP
         STOP
         END


C****************************************************************
C
C                                    FFT
C
C****************************************************************
      SUBROUTINE FFT(X,N,K)
         IMPLICIT INTEGER(A-Z)
         REAL*4 GAIN,PI2,ANG,RE,IM
         COMPLEX X(N),XTEMP,T,U(16),V,W
         LOGICAL NEW
         DATA PI2,GAIN,NO,KO/6.283185307,1.0,0,0/

         NEW=NO.NE.N
         IF(.NOT.NEW)GOTO 2
         L2N=0
         NO=1
1     L2N=L2N+1
      NO=NO+NO
         IF(NO.LT.N)GOTO 1
         GAIN=1.0/N
         ANG=PI2*GAIN
         RE=COS(ANG)
         IM=SIN(ANG)
2     IF(.NOT.NEW.AND.K*KO.GE.1)GOTO 4
      U(1)=CMPLX(RE,-SIGN(IM,FLOAT(K)))

         DO 3 I=2,L2N
3     U(I)=U(I-1)*U(I-1)

      KO=K
4     SBY2=N

      DO 7 STAGE=1,L2N
         V=U(STAGE)
         W=(1.0,0.0)
         S=SBY2
```

```
         SBY2=S/2
         DO 6 L=1,SBY2
          DO 5 I=1,N,S
           P=I+L-1
           Q=P+SBY2
           T=X(P)+X(Q)
           X(Q)=(X(P)-X(Q))*W
5      X(P)=T
6      W=W*V
7    CONTINUE

     DO 9 I=1,N
         INDEX=I-1
         JNDEX=0
         DO 8 J=1,L2N
          JNDEX=JNDEX+JNDEX
          ITEMP=INDEX/2
          IF(ITEMP+ITEMP.NE.INDEX)JNDEX=JNDEX+1
          INDEX=ITEMP
8      CONTINUE
     J=JNDEX+1
         IF(J.LT.I)GOTO 9
         XTEMP=X(J)
         X(J)=X(I)
         X(I)=XTEMP
9    CONTINUE

     IF(K.GT.0)RETURN

         DO 10 I=1,N
10     X(I)=X(I)*GAIN

     RETURN
         END
```

# Appendix C

## Linear Random Vibration

From PDE for an isotropic rectangular plate,

$$\rho h \frac{\partial^2 w}{\partial t^2} + D\nabla^4 w = p_0(t) \tag{C1}$$

For a simply supported boundary condition, the plate deflection and mode shape are

$$w(x, y, t) = \sum_m \sum_n q_{mn}(t)\phi_{mn}(x, y) \tag{C2}$$

$$\phi_{mn}(x, y) = \sin\left(\frac{m\pi x}{a}\right) \times \sin\left(\frac{m\pi y}{b}\right)$$

After substitution of Equation (C2) into Equation (C1) and applying the modal orthogonality condition, the modal equations are

$$\ddot{q}_{mn} + \omega_{mn}^2 q_{mn} = \frac{p_0(t)}{m_{mn}}, \qquad m, n = 1,3,5\ldots \tag{C3}$$

Adding a structural damping,

$$\ddot{q}_{mn} + 2\xi_{mn}\omega_{mn}\dot{q}_{mn} + \omega_{mn}^2 q_{mn} = \frac{p_0(t)}{m_{mn}} \tag{C4}$$

$$\omega_{mn} = \pi^2 \sqrt{\frac{D}{\rho h}} \left[\left(\frac{m}{a}\right)^2 + \left(\frac{n}{b}\right)^2\right] \text{ rad/sec} \tag{C5}$$

$$m_{mn} = \frac{mn\pi^2 \rho h}{16} \tag{C6}$$

where $\omega_{mn}$ and $m_{mn}$ are the natural frequency and modal mass, respectively.

The response to Equation (C4) is given by Equations (3-57) and (7-37) in reference [51],

$$E[q_{mn}^2] = \frac{\pi \times S_0(f)}{8m_{mn}^2 \xi_{mn} \omega_{mn}^3} \qquad (C7)$$

set mn=r and kl=s,

$$E[q_{mn}q_{kl}] = E[q_r q_s] = \frac{(\xi_r \omega_r + \xi_s \omega_s)S_0(f)}{m_r m_s \left[ (\omega_r^2 - \omega_s^2)^2 + 4\omega_r \omega_s (\xi_r \omega_r + \xi_s \omega_s)(\xi_r \omega_s + \xi_s \omega_r) \right]} \qquad (C8)$$

The root mean square of maximum deflection from Equation (C2) is

$$RMS(w_{max}) = \left\{ E\left[ \left( \sum_{r=1}^{n} q_r \right)^2 \right] \right\}^{1/2} \qquad (C9)$$

$$= \left\{ E[q_1^2] + E[q_2^2] + \ldots + 2E[q_1 q_2] + \cdots \right\}^{1/2}$$